4

Unsteady flows bounded by plane boundaries

The simplest unsteady flows involving plane boundaries, in which a single infinite boundary moves in its own plane, are associated with the names of Stokes (1851) and Rayleigh (1911). Consider a situation in which $\mathbf{v} = \{u(y, t), 0, 0\}$. Equation (1.12) is satisfied identically. Equations (1.9) and (1.10) then yield, respectively,

$$\frac{\partial u}{\partial t} = -\frac{1}{\rho}\frac{\partial p}{\partial x} + \nu\frac{\partial^2 u}{\partial y^2}, \tag{4.1}$$

$$\frac{\partial p}{\partial y} = 0. \tag{4.2}$$

Under the assumed conditions, the most general solution of equation (4.2) is $p = -\rho\{f(t) + xg(t)\}$, where f and g are arbitrary functions of t, so that (4.1) becomes

$$\frac{\partial u}{\partial t} = \nu\frac{\partial^2 u}{\partial y^2} + g(t); \tag{4.3}$$

differentiating this equation with respect to y, and introducing the vorticity $\boldsymbol{\omega} = (0, 0, \zeta)$ yields, as equation for ζ,

$$\frac{\partial \zeta}{\partial t} = \nu\frac{\partial^2 \zeta}{\partial y^2}. \tag{4.4}$$

Each of equations (4.3), (4.4) are analogous to the one-dimensional heat conduction equation. In (4.3) u plays the role of temperature with $g(t)$ representing an unsteady source of heat. The diffusion equation (4.4) has the vorticity ζ in the role of temperature with the equation representing diffusion of heat, though in a fluid-dynamical context diffusion of vorticity is a well established and valuable concept. We next consider solutions of equation (4.3), and its generalisation, in several physical contexts.

4.1 The oscillating plate

Consider first the classical problem of the flow induced when the infinite plane boundary $y = 0$ performs unidirectional oscillations, frequency ω, in its own plane such that $u(0, t) = U_0 \cos \omega t$ where U_0 is a constant. With $g(t) \equiv 0$ we seek a solution in which $u = U_0 e^{i\omega t} F(y)$ where, from (4.3), F satisfies

$$\nu F'' - i\omega F = 0, \tag{4.5}$$

with

$$F(0) = 1, \quad F \to 0 \quad \text{as} \quad y \to \infty. \tag{4.6}$$

The solution of (4.5) subject to (4.6) is $F(y) = \exp\{-(1 + i)(\omega/2\nu)^{1/2} y\}$ so that, taking the real part, we have

$$u = U_0\, e^{-(\omega/2\nu)^{1/2} y} \cos\{\omega t - (\omega/2\nu)^{1/2} y\}. \tag{4.7}$$

The shear stress exerted on the plate is given by

$$\mu \frac{\partial u}{\partial y}\bigg|_{y=0} = U_0 (\rho\mu\omega)^{1/2} \cos(\omega t + 5\pi/4),$$

which is seen to differ in phase from the velocity of the boundary.

The solution (4.7) shows that vorticity, of alternating sign, created at the boundary propagates from it in a wave-like manner with speed $(2\omega\nu)^{1/2}$. This viscous wave decays in amplitude and the whole motion is confined to a layer of thickness $O\{(\nu/\omega)^{1/2}\}$, often referred to as the 'Stokes layer'. If the fluid is confined by an upper, stationary, boundary at $y = h$, say, then the condition as $y \to \infty$ is replaced by $F(h) = 0$ with corresponding solution

$$\begin{aligned} u = \frac{U_0}{2(\cosh 2\lambda h - \cos 2\lambda h)} \{ & e^{-\lambda(y-2h)} \cos(\omega t - \lambda y) \\ & + e^{\lambda(y-2h)} \cos(\omega t + \lambda y) - e^{-\lambda y} \cos(\omega t - \lambda y + 2\lambda h) \\ & - e^{\lambda y} \cos(\omega t + \lambda y - 2\lambda h)\} \end{aligned}$$

where $\lambda = (\omega/2\nu)^{1/2}$.

The effect of suction on the Stokes-layer solution has been considered by both Stuart (1955) and Debler and Montgomery (1971). If we assume that $\mathbf{v} = \{u(y, t), v(y), 0\}$ then equation (1.12) shows that $\partial v/\partial y = 0$ and we infer that $v = \text{constant} = -V$, say, where V is the suction velocity. The analogue of equation (4.3), again with $g = 0$, is then seen to be, from (1.9),

$$\frac{\partial u}{\partial t} - V \frac{\partial u}{\partial y} = \nu \frac{\partial^2 u}{\partial y^2} \tag{4.8}$$

with, as before, $u(0,t) = U_0 \cos \omega t$ and $u \to 0$ as $y \to \infty$. If we seek a solution analogous to (4.7) in the form

$$u = U_0 \, \mathrm{e}^{-ay} \cos(\omega t + by), \tag{4.9}$$

then direct substitution in equation (4.8) yields for the constants a and b

$$a = \left(\frac{\omega}{2\nu}\right)^{1/2} \left[\left\{ 1 + \left(\frac{V^2}{4\omega\nu}\right)^2 \right\}^{1/2} - \frac{V^2}{4\omega\nu} \right]^{-1/2} + \frac{V}{2\nu}, \tag{4.10}$$

$$b = -\left(\frac{\omega}{2\nu}\right)^{1/2} \left[\left\{ 1 + \left(\frac{V^2}{4\omega\nu}\right)^2 \right\}^{1/2} - \frac{V^2}{4\omega\nu} \right]^{1/2}. \tag{4.11}$$

Debler and Montgomery show that if a steady transverse velocity, W, is introduced such that now $\mathbf{v} = \{u(y,t), -V, w(y)\}$, then u is unchanged, as in (4.9), and the solution of equation (1.11) is the asymptotic suction profile analysed in chapter 2, namely

$$w = W(1 - \mathrm{e}^{-Vy/\nu}).$$

The investigation by Debler and Montgomery was motivated by a particular papermaking device that oscillates laterally as a dilute mixture of water and wood pulp is carried along it. In their study they also utilised the ideas based on the Stokes solution for the case in which a liquid film is adjacent to the oscillating boundary, with a gaseous medium above it. The solution is completed by ensuring continuity of velocity and stress at the two-phase interface. Stuart was concerned with the effects of streamwise fluctuations on a steady flow speed U_1, say, that corresponds to the asymptotic suction profile. In that case the porous boundary is at rest and streamwise fluctuations $U_0 \cos \omega t$ are introduced. The solution for the velocity component $u(y,t)$ is readily seen to be

$$u = U_1(1 - \mathrm{e}^{-Vy/\nu}) + U_0\{\cos \omega t - \mathrm{e}^{-ay} \cos(\omega t + by)\}, \tag{4.12}$$

where a and b are given by (4.10) and (4.11). Kelly (1965) has also included the effect of a time-dependent suction velocity.

4.2 Impulsive flows

The prototype impulsive flow arises when the infinite plane is set in motion with constant velocity in its own plane. This flow was analysed by Stokes (1851) and Rayleigh (1911). Watson (1955), seeking a generalisation of this flow, considered situations in which the boundary velocity $U(t)$ leads to solutions of equation (4.3), in the absence of the source term $g(t)$, which are self-similar. He found that there are two possibilities namely

$$U(t) = At^{\alpha}, \quad U(t) = A\,\mathrm{e}^{\omega t}. \tag{4.13}$$

For the first of these we have

$$u = At^{\alpha} f(\eta) \quad \text{where} \quad \eta = y/2(\nu t)^{1/2}, \tag{4.14}$$

and from (4.3) we have, as the equation for f,

$$f'' + 2\eta f' - 4\alpha f = 0, \tag{4.15}$$

together with

$$f(0) = 1, \quad f \to 0 \quad \text{as} \quad \eta \to \infty. \tag{4.16}$$

The solution of equation (4.15), subject to (4.16), may be written as

$$\begin{aligned} f &= 2^{2\alpha}\Gamma(\alpha+1)g_{\alpha}(\eta) \quad \text{where} \\ g_{\alpha} &= 2^{(1/2)-\alpha}\pi^{-1/2} \ \exp(-\eta^2/2)D_{-2\alpha-1}(\sqrt{2}\eta), \end{aligned} \tag{4.17}$$

where $\Gamma(x)$ is the gamma function and $D_n(x)$ the parabolic cylinder function. The function $g_{\alpha}(\eta)$ has the properties that

$$g'_{\alpha}(\eta) = -g_{\alpha-1/2}(\eta), \quad g_0(\eta) = 1 - \mathrm{erf}(\eta), \quad g_{\alpha}(0) = \frac{2^{-2\alpha}}{\Gamma(\alpha+1)}. \tag{4.18}$$

In figure 4.1 we show the velocity function $f(\eta)$ for various values of α. The case $\alpha = 0$ is the classical case, first considered by Stokes, corresponding to the situation in which the plane moves with constant velocity from the initial instant.

The shear stress exerted on the plane is given by

$$\mu\frac{\partial u}{\partial y}\bigg|_{y=0} = \frac{1}{2}A(\rho\mu)^{1/2}t^{\alpha-1/2}f'(0) = -A(\rho\mu)^{1/2}t^{\alpha-1/2}\frac{\Gamma(\alpha+1)}{\Gamma(\alpha+1/2)},$$

and in figure 4.2 we plot $f'(0) = -2\Gamma(\alpha+1)/\,\Gamma(\alpha+\frac{1}{2})$ as a function of α.

The effect of suction on this class of flows, with the wall suction $V(t) \propto t^{-1/2}$, has been considered by Hasimoto (1957).

The second possibility shown in equation (4.13) leads to a distribution of velocity $u(y,t) = A\,\mathrm{e}^{\omega t} f(y)$ from which it readily emerges that $f = \exp\{-(\omega/\nu)^{1/2}y\}$. This solution was first discussed by Görtler (1944), and may be interpreted as a flow in which the plane is set into motion from a state of rest at $t = -\infty$.

From the first class of these solutions, we see from (4.14) that the vorticity created at the plane $y = 0$, a vortex sheet at the initial instant, diffuses without

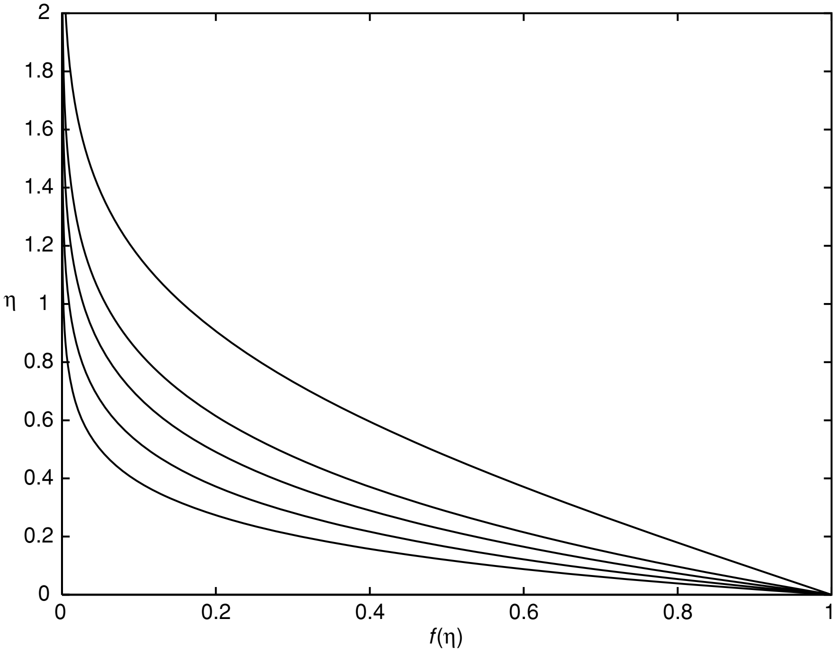

Figure 4.1 The velocity function $f(\eta)$, when the boundary moves with speed At^α, for values of $\alpha = 0$ (uppermost), 1, 2, 4, 8.

bound into the main body of the fluid to a distance $O\{(\nu t)^{1/2}\}$ at time t. By contrast, for the second type of solution although the vorticity intensifies at an exponential rate with respect to time it is constrained to a region of thickness $O\{(\nu/\omega)^{1/2}\}$ as in the Stokes layer.

Other planar impulsive flows are outlined by Berker (1963) including the following.

4.2.1 Applied body force

If a body force $\mathbf{F} = k\mathbf{i}$ is applied to the fluid which is at rest initially, with the boundary $y = 0$ at rest, then $u(y, t)$ satisfies equation (4.3) with $g(t)$ replaced by k, and $u(y, 0) = 0$, $0 < y < \infty$, $u(0, t) = 0$, $0 < t < \infty$. Setting $u = kt + \bar{u}$ then shows that $\bar{u}$ satisfies

$$\frac{\partial \bar{u}}{\partial t} = \nu \frac{\partial^2 \bar{u}}{\partial y^2}, \tag{4.19}$$

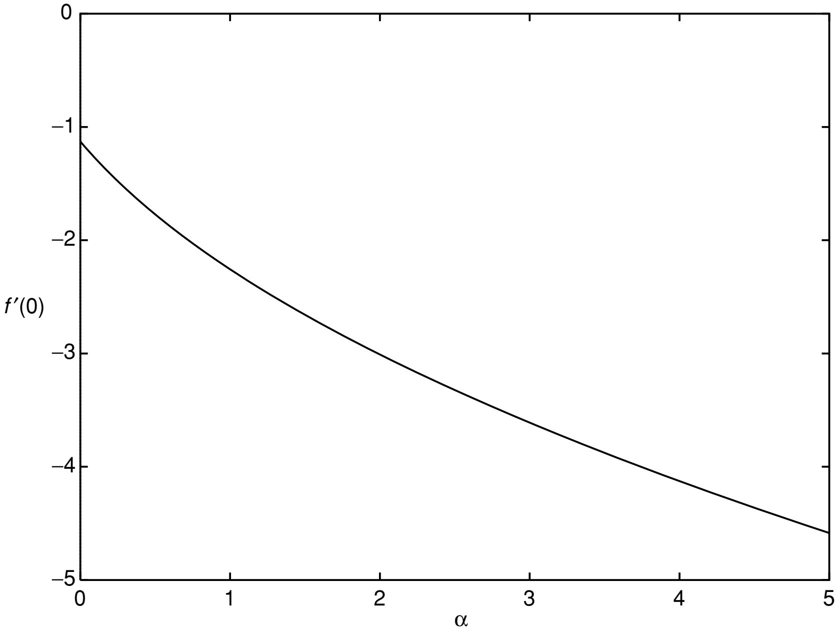

Figure 4.2 The shear-stress function $f'(0)$ for the class of flows illustrated in figure 4.1.

together with

$$\bar{u}(y,0) = 0, \quad 0 < y < \infty, \quad \bar{u}(0,t) = -kt, \quad 0 < t < \infty;$$
$$\bar{u} \to 0 \quad \text{as} \quad y \to \infty. \tag{4.20}$$

The problem posed by equations (4.19), (4.20) is a special case of those investigated by Watson, considered above, with $\alpha = 1$. The solution is given by (4.14), (4.17) with $A = -k$ so that, finally,

$$u = kt\{1 - 2^{-3/2}\pi^{-1/2}\exp(-\eta^2/2)D_{-3}(\sqrt{2}\eta)\}.$$

4.2.2 Applied shear stress

An alternative to inducing a motion in the bulk of the fluid by setting the plane boundary $y = 0$ into motion is to apply a shear stress at the boundary, so that $\mu\, \partial u/\partial y|_{y=0} = -T$ with, for example, T constant. If we write

$$\bar{u} = \mu \frac{\partial u}{\partial y} \tag{4.21}$$

then $\bar{u}$ satisfies equation (4.19) and the conditions (4.20) except that the condition at $y = 0$ is replaced by $\bar{u}(0, t) = -T$, $0 < t < \infty$. The problem for $\bar{u}$ is, then, the classical problem of an impulsively moved plane with constant speed. The solution we infer from (4.14) and (4.18), with $\alpha = 0$, as

$$\bar{u} = T\left\{\frac{2}{\sqrt{\pi}}\int_0^{\eta} \mathrm{e}^{-s^2}\mathrm{d}s - 1\right\} \quad \text{where} \quad \eta = y/2(\nu t)^{1/2}. \tag{4.22}$$

From this expression we deduce that

$$u = \frac{T}{\mu}\left[2\left(\frac{\nu t}{\pi}\right)^{1/2}\mathrm{e}^{-y^2/4\nu t} + y\left\{\mathrm{erf}\left(\frac{y}{2(\nu t)^{1/2}}\right) - 1\right\}\right], \tag{4.23}$$

with $u(0, t) = 2T(t/\rho\mu\pi)^{1/2}$. Berker (1963) explores the possibility that the solution (4.23) may find application in the study of wind-driven marine currents.

4.2.3 Diffusion of a vortex sheet

As a preliminary we note that $u = t^{-1/2}\exp(-y^2/4\nu t)$ is a solution of equation (4.3) in the absence of the source term and that, therefore, so also is

$$u = \frac{1}{2(\pi\nu t)^{1/2}}\int_{-\infty}^{\infty} \mathrm{e}^{-(s-y)^2/4\nu t} f(s)\,\mathrm{d}s, \tag{4.24}$$

a solution that has the property $u \to f(y)$ as $t \to 0$, for $-\infty < y < \infty$. Consider then the case when the initial velocity distribution is given as

$$u = \begin{cases} u_0, & \text{for} \quad y > 0, \\ -u_0, & \text{for} \quad y < 0, \end{cases}$$

where u_0 is a constant. This distribution implies the presence of a vortex sheet at $y = 0$ at the initial instant. From equation (4.24) we then have

$$u = \frac{u_0}{2(\pi\nu t)^{1/2}}\left(\int_0^{\infty} \mathrm{e}^{-(s-y)^2/4\nu t}\,\mathrm{d}s - \int_0^{\infty} \mathrm{e}^{-(s+y)^2/4\nu t}\,\mathrm{d}s\right). \tag{4.25}$$

From the solution (4.25) we find the normal component of vorticity as

$$\zeta = -\frac{u_0}{(\pi\nu t)^{1/2}}\mathrm{e}^{-y^2/4\nu t}. \tag{4.26}$$

Distributions of this vorticity, at various times, as the vortex sheet diffuses are shown in figure 4.3. The total vorticity remains constant, of course, and equal to $-2u_0$ per unit length.

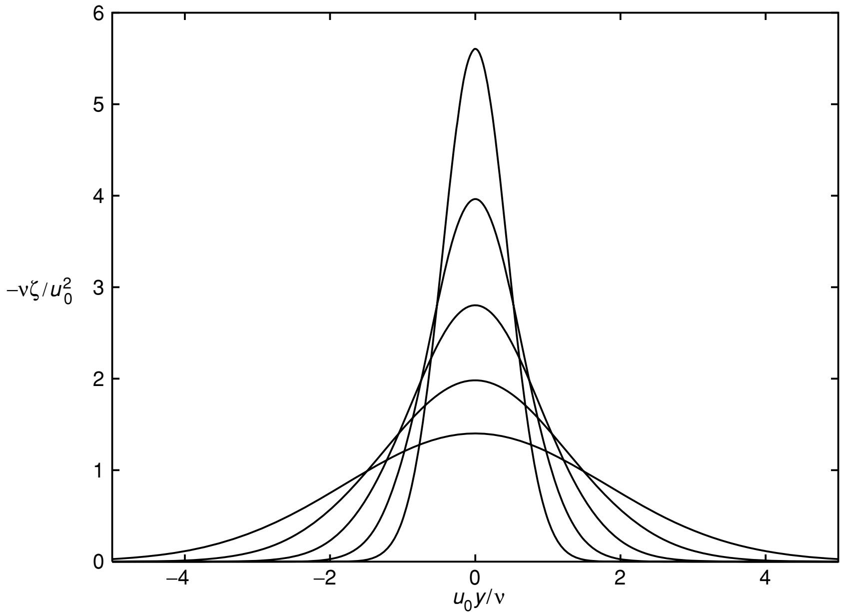

Figure 4.3 The vorticity in a diffusing vortex sheet for values of $\bar{t} = u_0^2 t/\nu = 0.1$ (uppermost), 0.2, 0.4, 0.8, 1.6.

4.3 More general flows

Watson (1958) uses the asymptotic suction profile as a steady base flow on which unsteady motions are superposed, whilst Hasimoto (1957) has considered situations, with uniform suction, for which the free stream $U(t) \equiv 0$ for $t < 0$. With $v \equiv -V$ and a free stream $U(t) = U_1\{1 + f(t)\}$, where f is given, flowing past the fixed boundary $y = 0$ we have, as equation for $u(y, t)$,

$$\frac{\partial u}{\partial t} - V\frac{\partial u}{\partial y} = \frac{\mathrm{d}U}{\mathrm{d}t} + \nu\frac{\partial^2 u}{\partial y^2}. \tag{4.27}$$

The solution of this equation may be written as

$$u = U_1(1 - \mathrm{e}^{-Vy/\nu}) + U_1 g(y, t)$$

where g satisfies, from (4.27),

$$\frac{\partial^2 g}{\partial \eta^2} + \frac{\partial g}{\partial \eta} - \frac{\partial g}{\partial \tau} = -\frac{\mathrm{d}f}{\mathrm{d}\tau}, \tag{4.28}$$

where $\eta = Vy/\nu$ and $\tau = V^2 t/\nu$. To solve (4.28), Watson introduces the two-sided Laplace transform

$$\tilde{g}(\eta, s) = s^2 \int_{-\infty}^{\infty} \mathrm{e}^{-s\tau} g(\eta, \tau)\,\mathrm{d}\tau,$$

so that $\tilde{g}$ satisfies, from (4.28),

$$\frac{\partial^2 \tilde{g}}{\partial \eta^2} + \frac{\partial \tilde{g}}{\partial \eta} - s\tilde{g} = -s\tilde{f}. \tag{4.29}$$

The appropriate solution of equation (4.29) is $\tilde{g} = \tilde{f}(1 - \mathrm{e}^{-k\eta})$ where $k = \{1 + (1+4s)^{1/2}\}/2$. For a prescribed $f(t)$, $\tilde{f}$ is known, and using the convolution-product rule to find the inverse of $\tilde{g}$ we have, finally,

$$u = U_1 \left[1 - \mathrm{e}^{-\eta} + f(\tau) - \frac{\eta\,\mathrm{e}^{-\eta/2}}{4\sqrt{\pi}} \int_0^{\infty} \lambda^{-3/2} f(\tau - \lambda) \right.$$
$$\left. \times \exp\left\{ - \left(\lambda + \frac{\eta^2}{16\lambda} \right) \right\} \mathrm{d}\lambda \right]. \tag{4.30}$$

From (4.30), with $f(t) = \cos \omega t$, the result of Stuart (1955) set out in equation (4.12) may be recovered. Watson also considers impulsive situations. For example if $U = U_1\{1 + H(\tau)\Delta\}$, where Δ is a constant and $H(\tau)$ the Heaviside unit function, then equation (4.30) yields

$$u = U_1 \left[1 - \mathrm{e}^{-\eta} + H(\tau)\Delta \left\{ 1 - \frac{1}{2}\mathrm{e}^{-\eta}\mathrm{erfc}\left(\frac{\eta}{4\tau^{1/2}} - \tau^{1/2} \right) \right. \right.$$
$$\left. \left. - \frac{1}{2}\mathrm{erfc}\left(\frac{\eta}{4\tau^{1/2}} + \tau^{1/2} \right) \right\} \right]. \tag{4.31}$$

A multi-step change in free-stream speed, $U = U_1[1 + \{H(\tau) - H(\tau - \tau_0)\}\Delta]$, which reduces it to the original value U_1 after an interval τ_0 is also considered. The shear stress at the boundary, $\tau_w = \mu \partial u/\partial y|_{y=0}$ is given, from (4.31), as

$$\frac{\tau_w}{\rho U_1 V} = 1 + \frac{1}{2} H(\tau)\Delta \left\{ 1 + \mathrm{erf}(\tau^{1/2}) + \frac{\mathrm{e}^{-\tau}}{(\pi\tau)^{1/2}} \right\}. \tag{4.32}$$

A further example by Watson has the free stream accelerating, from some initial instant, such that $U = U_1\{1 + H(\tau)\Delta\tau\}$ and the velocity distribution is given from equation (4.30) as

$$u = U_1 \left[1 - \mathrm{e}^{-\eta} + \frac{1}{8} H(\tau)\Delta \left\{ 8\tau - (4\tau - \eta)\,\mathrm{erfc}\left(\frac{\eta}{4\tau^{1/2}} - \tau^{1/2} \right) \right. \right.$$
$$\left. \left. - (4\tau + \eta)\,\mathrm{erfc}\left(\frac{\eta}{4\tau^{1/2}} + \tau^{1/2} \right) \right\} \right], \tag{4.33}$$

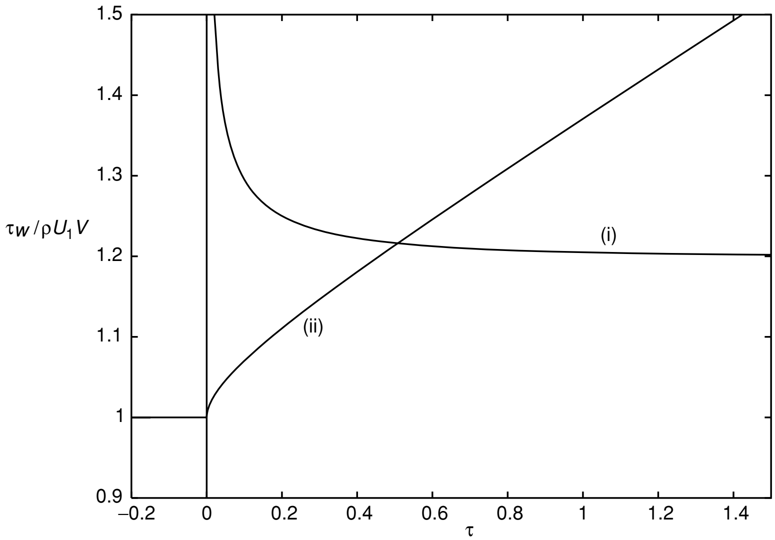

Figure 4.4 The shear stress $\tau_w/\rho U_1 V$ (i) from equation (4.32) following an impulsive change in free-stream speed, and (ii) from equation (4.33) when the free stream accelerates at $t = 0$.

from which the boundary shear stress is given as

$$\frac{\tau_w}{\rho U_1 V} = 1 + \frac{1}{2}H(\tau)\Delta\left\{\tau + \frac{1}{2}\mathrm{erf}(\tau^{1/2}) + \left(\frac{\tau}{\pi}\right)^{1/2}\mathrm{e}^{-\tau} + \tau\,\mathrm{erf}(\tau^{1/2})\right\}. \tag{4.34}$$

Watson also considers a multiple acceleration that brings the free-stream speed back to its uniform value U_1. In all of these situations, following the change in free-stream conditions, additional vorticity is created at the boundary, initially confined to a layer of thickness $O\{(\nu t)^{1/2}\}$, as in the impulsive flows considered in section 4.2.

The boundary shear stresses for the examples detailed above, given by equations (4.32) and (4.34) are shown in figure 4.4.

As a final example Watson studies the case of a decaying oscillation superposed on the free stream at the initial instant such that $U = U_1\{1 + H(\tau)\Delta\,\mathrm{e}^{-a\tau}\sin b\tau\}$ where a $(a > 0)$ and b are constants.

4.4 The angled flat plate

The classical problem of the impulsive motion of an infinite plate, in its own plane, has been treated in section 4.2. The case when the plate is 'bent', so that two semi-infinite planes intersect, along the x-axis, say, at an angle α ($0 < \alpha \leq 2\pi$) has been considered by Sowerby (1951), Hasimoto (1951) and Sowerby and Cooke (1953). The angled plate is set into motion impulsively, at time $t = 0$, with uniform speed U_0 in the x-direction. It proves convenient to introduce cylindrical polar co-ordinates which in this case, for consistency of notation with sections 4.1 and 4.2, are defined such that $z = r\cos\theta$, $y = r\sin\theta$. We assume $\mathbf{v} = \{u(r, \theta, t), 0, 0\}$ so that the continuity equation is satisfied identically and, in the absence of any pressure gradient, the equation satisfied by $u(r, \theta, t)$ may be inferred from equation (1.21) as

$$\frac{\partial u}{\partial t} = \nu\left(\frac{\partial^2 u}{\partial r^2} + \frac{1}{r}\frac{\partial u}{\partial r} + \frac{1}{r^2}\frac{\partial^2 u}{\partial \theta^2}\right). \tag{4.35}$$

The boundary conditions require

$$u \equiv 0, \quad r > 0 \quad \text{at} \quad t = 0,$$

and for $t > 0$,

$$u = U_0 \ \text{ for } \ \theta = 0, \alpha, \ \text{ all } \ r; \quad u \to 0 \ \text{ as } \ r \to \infty \ \text{ for } \ 0 < \theta < \alpha. \tag{4.36}$$

The most detailed investigation of this problem has been carried out by Sowerby and Cooke who, drawing upon an analogous heat conduction problem, see for example Carslaw and Jaeger (1947), find an infinite series solution for $t > 0$ of (4.35), subject to the boundary conditions (4.36), as

$$u = U_0\left\{1 - \frac{2}{\alpha}\sum_{n=0}^{\infty}\sin s\theta\,\frac{\Gamma(\frac{1}{2}s)}{\Gamma(s+1)}\eta^s\,\mathrm{e}^{-\eta^2}\,{}_1F_1\left(\tfrac{1}{2}s + 1; s + 1 : \eta^2\right)\right\}, \tag{4.37}$$

where $s = (2n+1)\pi/\alpha$, $\eta = r/2(\nu t)^{1/2}$ and ${}_1F_1$ is the confluent hypergeometric function.

The important special case $\alpha = 2\pi$ was considered earlier by Howarth (1950), and (4.37) recovers his solution as $\alpha \to 2\pi$. In that particular case the configuration is one in which a semi-infinite plate is moved impulsively in its own plane parallel to its edge. Both Sowerby and Cooke, and Howarth, discuss alternative representations of the solution (4.37). However, the series (4.37) converges rapidly close to the intersection $r = 0$ and, in particular, Howarth shows that for his case of $\alpha = 2\pi$ the skin friction, close to the edge, is given by

$$\mu\left.\frac{\partial u}{\partial y}\right|_{y=0} \approx -0.46\mu U_0(\nu t)^{-3/4}r^{1/2}.$$

The 'edge effect' is shown by Howarth to be confined to a region of scale $O\{(\nu t)^{1/2}\}$. Beyond this, as $r \to \infty$ along the plate, the classical solution readily emerges.

In his earlier paper Sowerby (1951) had confined attention to the case where $\alpha = \pi/m$, where $m \geq 1$ is an integer, with solution $u_m(r, \theta, t)$. Relatively simple solutions emerge. For example

$$u_1 = U_0\{1 - \mathrm{erf}(\eta \sin\theta)\},$$
$$u_2 = U_0\{1 - \mathrm{erf}(\eta \cos\theta)\mathrm{erf}(\eta \sin\theta)\},$$
$$u_3 = U_0[1 - \mathrm{erf}(\eta \sin\theta) - \mathrm{erf}\{\eta \sin(\pi/3 - \theta)\} + \mathrm{erf}\{\eta \sin(2\pi/3 - \theta)\}],$$

the first of which is, of course, the classical infinite flat plate solution.

In this category of solution we might also mention the work of Levine (1957) who considers the case of an infinite strip, of width $2a$, set into motion with uniform speed U_0.

4.5 Unsteady plate stretching

Devi, Takhar and Nath (1986) have extended the analysis of Wang (1984), for steady three-dimensional flow due to an impermeable stretching plate, to include a particular time dependence. It proves convenient, as in section 2.5.4 to introduce a slight change of notation such that x, y are co-ordinates in the plane, with z perpendicular to it. Then, if the boundary velocities are given by $u = kx(1 - \lambda kt)^{-1}$, $v = ly(1 - \lambda kt)^{-1}$, a self-similar solution is available in which

$$u = kx(1 - \lambda kt)^{-1} f'(\eta), \quad v = ky(1 - \lambda kt)^{-1} g'(\eta),$$
$$w = -(k\nu)^{1/2}(1 - \lambda kt)^{-1/2}\{f(\eta) + g(\eta)\} \tag{4.38}$$

where $\eta = (k/\nu)^{1/2}(1 - \lambda kt)^{-1/2} z$. The velocity components in (4.38) satisfy the continuity equation, and equations (1.9), (1.10) then give, as equations for f and g,

$$f''' + (f + g)f'' - f'^2 - \lambda\left(f' + \tfrac{1}{2}\eta f''\right) = 0,$$

$$g''' + (f + g)g'' - g'^2 - \lambda\left(g' + \tfrac{1}{2}\eta g''\right) = 0,$$

together with

$$f(0) = g(0) = 0, \quad f'(0) = 1, \quad g'(0) = r; \quad f', g' \to 0 \quad \text{as} \quad \eta \to \infty,$$

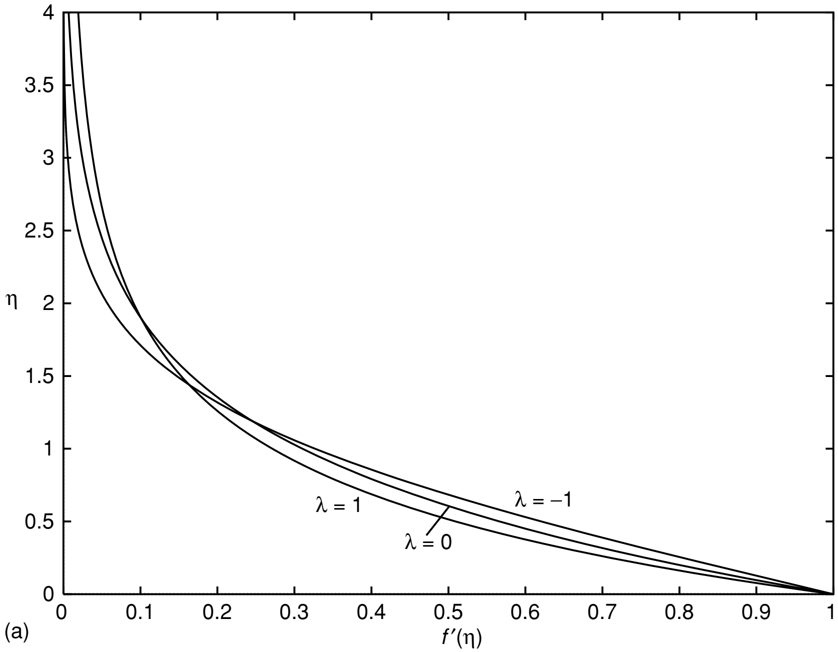

Figure 4.5 (a) Velocity profiles $f'(\eta)$ for $r = \frac{1}{2}$ and $\lambda = -1, 0, 1$. (b) As (a) for the profiles $g'(\eta)$.

where $r = l/k$. This system of equations has been integrated numerically by Devi *et al.* and we present representative velocity profiles in figure 4.5. It may be noted that for the range of decelerating/accelerating flows for which $-1 \leq \lambda \leq 1$ the velocity profiles $f'(\eta)$, $g'(\eta)$ differ little from the steady state stretching solution of Wang (1984).

An interpretation of this solution for $\lambda > 0$ is that of a flow starting from rest at $t = -\infty$ which then accelerates to become unbounded at $t = (\lambda k)^{-1}$ within a layer of vanishing thickness. Devi *et al.* suggest it may find application in extrusion processes.

4.6 Beltrami flows and their generalisation

As we have already noted in section 2.2 Beltrami flows are flows for which $\mathbf{v} \wedge \boldsymbol{\omega} = \mathbf{0}$, and for steady situations, except for the case $\boldsymbol{\omega} \equiv \mathbf{0}$, such flows can only be sustained through the action of a non-conservative body force. For unsteady flow, in the absence of any body force, $\mathbf{v} \wedge \boldsymbol{\omega} = \mathbf{0}$ implies

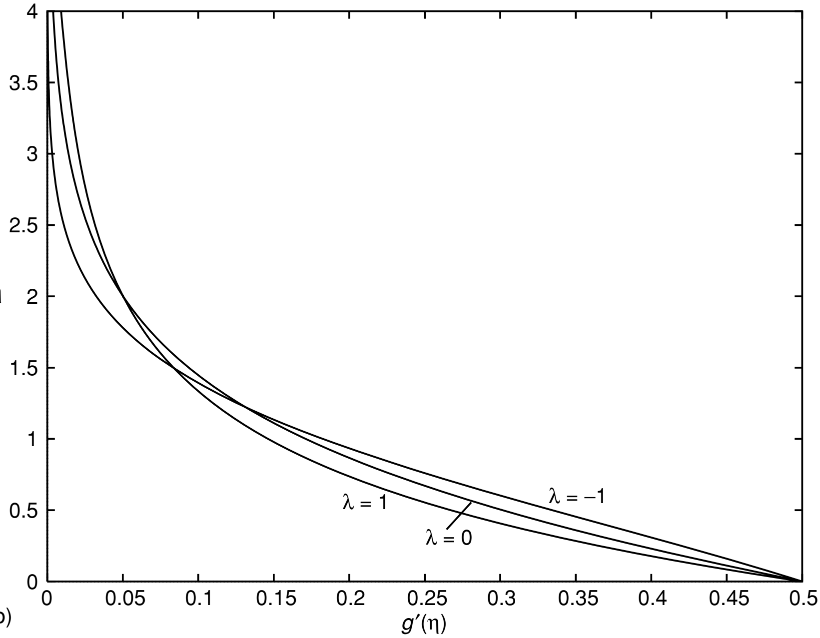

(b)

Figure 4.5 (*cont.*)

$$\frac{\partial \boldsymbol{\omega}}{\partial t} = \nu \nabla^2 \boldsymbol{\omega}, \tag{4.39}$$

with

$$\boldsymbol{\omega} = c(\mathbf{x}, t)\mathbf{v}. \tag{4.40}$$

Equation (4.40) shows immediately that such Beltrami flows can be neither planar nor axisymmetric. Setting

$$\mathbf{v} = \mathrm{e}^{-c^2 \nu t}\mathbf{f}(\mathbf{x}), \tag{4.41}$$

where c is a constant, Trkal (1919) has shown that both equations (4.39), (4.40) will be satisfied if

$$\nabla \wedge \mathbf{f} = c\mathbf{f}, \tag{4.42}$$

and Berker (1963) has obtained a solution for $\mathbf{f}$ as

$$\mathbf{f} = -\frac{1}{\sqrt{2}}\left(\cos\frac{cx}{\sqrt{2}}\sin\frac{cy}{\sqrt{2}}, \quad -\sin\frac{cx}{\sqrt{2}}\cos\frac{cy}{\sqrt{2}}, \quad -\sqrt{2}\cos\frac{cx}{\sqrt{2}}\cos\frac{cy}{\sqrt{2}}\right). \tag{4.43}$$

As for steady flows considered in section 2.2, a generalisation of these Beltrami flows requires

$$\nabla \wedge (\mathbf{v} \wedge \boldsymbol{\omega}) = \mathbf{0} \tag{4.44}$$

and $\boldsymbol{\omega}$ still satisfying equation (4.39). With $\boldsymbol{\omega} = (0, 0, \zeta)$ and $\mathbf{v} = \nabla \wedge (\psi \mathbf{k})$ as in section 2.2, ζ and the stream function ψ are, from (4.44) again related by equation (2.16), whose solution may now be written as

$$\zeta = -f(\psi, t). \tag{4.45}$$

As before, see equation (1.15), we have

$$\frac{\partial^2 \psi}{\partial x^2} + \frac{\partial^2 \psi}{\partial y^2} = -\zeta \tag{4.46}$$

and equation (4.39) requires

$$\frac{\partial \zeta}{\partial t} = \nu \left(\frac{\partial^2 \zeta}{\partial x^2} + \frac{\partial^2 \zeta}{\partial y^2} \right) \tag{4.47}$$

so that an exact solution of the Navier–Stokes equations results when equations (4.45) to (4.47) are compatible.

A particularly simple form of (4.45) is $\zeta = \alpha\psi$. If we then write $\psi = A\,\mathrm{e}^{\beta t}\,\Phi(x, y)$ both equations (4.46), (4.47) will be satisfied provided $\beta = -\nu\alpha$ and Φ satisfies

$$\frac{\partial^2 \Phi}{\partial x^2} + \frac{\partial^2 \Phi}{\partial y^2} + \alpha\Phi = 0.$$

Separation of variables, so that $\Phi(x, y) = F(x)G(y)$, then gives

$$\frac{\mathrm{d}^2 F}{\mathrm{d}x^2} G + F \frac{\mathrm{d}^2 G}{\mathrm{d}y^2} + \alpha F G = 0. \tag{4.48}$$

Three special solutions of (4.48) are the following.

(i) $F = \cos ax$, $G = \cos by$. In that case $\alpha = a^2 + b^2$ and

$$\psi = A \cos ax \cos by\, \mathrm{e}^{-\nu(a^2+b^2)t}. \tag{4.49}$$

This result was obtained by Taylor (1923) for the special case $a = b$. It may be interpreted as a double array of vortices which decay exponentially with time; the decay rate increases as the scale of the vortices decreases. An example is shown in figure 4.6.

Whilst there is a superficial similarity between (4.41) and (4.49) the essential difference should be noted, namely that in Trkal's solution $\mathbf{v} \wedge \boldsymbol{\omega} = \mathbf{0}$, whilst in Taylor's $\mathbf{v}.\boldsymbol{\omega} = 0$.

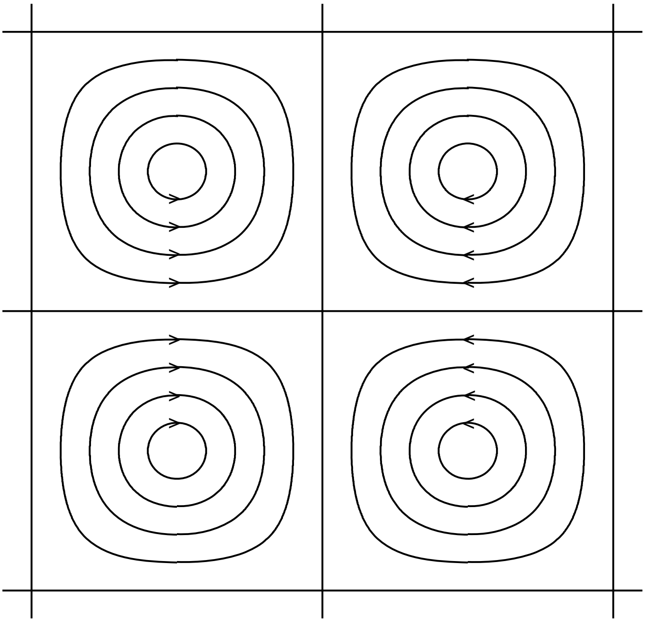

Figure 4.6 Instantaneous streamlines for the double array of vortices considered by Taylor (1923).

(ii) $F = \cosh ax$, $G = \cos by$. For this case $\alpha = b^2 - a^2$ and

$$\psi = A \cosh ax \cos by \, e^{\nu(a^2 - b^2)t}. \tag{4.50}$$

Wang (1966) presents this solution as the viscous analogue of Kelvin's 'cat's eye' vortices, which decay or increase without bound depending upon $a < b$ or $a > b$. A typical streamline pattern is shown in figure 4.7.

(iii) $F = \sinh ax$, $G = \sinh by$. We have $\alpha = -(a^2 + b^2)$ and so

$$\psi = A \sinh ax \sinh by \, e^{\nu(a^2 + b^2)t}. \tag{4.51}$$

Equation (4.51) is a solution that grows without bound, and is interpreted by Wang (1966) as the impingement of two rotational flows. For $|ax|, |by| \ll 1$ we have $\psi \propto xy \, e^{\nu(a^2+b^2)t}$, a time-varying classical stagnation-point flow.

Wang (1989a) generalises the above by writing

$$\zeta = \alpha\{\psi - U(t)y\} \tag{4.52}$$

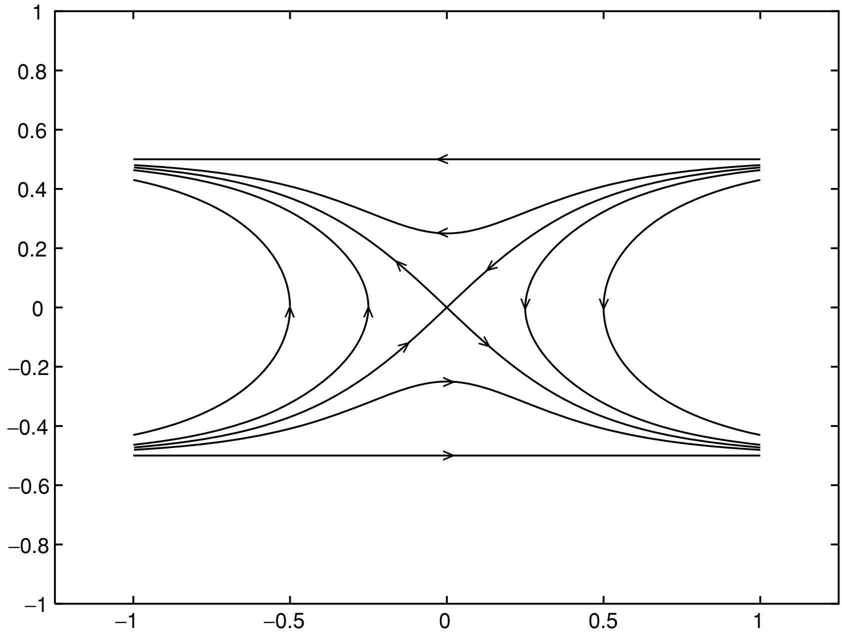

Figure 4.7 An example of the streamline pattern for Wang's (1966) solution, equation (4.50), with $a = b = \pi$ which corresponds, in fact, to a steady state.

so that the vorticity equation (1.17) then yields, as the equation for ψ,

$$\frac{\partial \psi}{\partial t} - \frac{\mathrm{d}U}{\mathrm{d}t} y + U \frac{\partial \psi}{\partial x} = \nu \nabla^2 \psi. \tag{4.53}$$

If we now write

$$\psi = U(t) y + V(t) F(x, y) \tag{4.54}$$

then from equation (4.46), we have, as the equation for F,

$$\nabla^2 F + \alpha F = 0.$$

We take as the solution of this equation

$$F = B \sin \frac{2\pi y}{h} \mathrm{e}^{-(4\pi^2/h^2 - \alpha)^{1/2} x}. \tag{4.55}$$

To complete the solution for ψ in (4.54) we find, from equation (4.53),

$$\frac{\mathrm{d}V}{\mathrm{d}t} - \left(\frac{4\pi^2}{h^2} - \alpha \right)^{1/2} UV + \alpha \nu V = 0, \tag{4.56}$$

so that V is determined in terms of U as

$$V = \exp\left\{\left(\frac{4\pi^2}{h^2} - \alpha\right)^{1/2} \int U\,\mathrm{d}t - \alpha\nu t\right\}. \tag{4.57}$$

For the special case $V = U$ the solution of (4.56) is

$$U = \frac{\alpha\nu}{(4\pi^2/h^2 - \alpha)^{1/2}(1 - \mathrm{e}^{\alpha\nu t})}, \tag{4.58}$$

a result that was anticipated by Berker (1963). If, for example, we now set

$$\alpha = \frac{R(R^2 + 16\pi^2)^{1/2} - R^2}{2h^2} > 0,$$

where $R = U_0 h/\nu$ is a Reynolds number based on a representative velocity U_0, then from (4.54), (4.55) and (4.58) the solution is

$$\psi = \frac{\alpha\nu}{(4\pi^2/h^2 - \alpha)^{1/2}(1 - \mathrm{e}^{\alpha\nu t})}\left[y + B\sin\frac{2\pi y}{h}\right.$$
$$\left.\times \exp\left[\left\{R - \sqrt{(R^2 + 16\pi^2)}\right\} x/2h\right]\right]. \tag{4.59}$$

As $t \to -\infty$ this solution, with B arbitrary, approaches the steady solution of Kovásznay, as in equation (2.27), and decays as $t \to \infty$.

Wang (1989a) also considers, with $V \neq U$, a generalisation of his solution (Wang (1966)) of a uniform stream encountering a diverging counterflow which has been outlined in section 2.2.1.

4.7 Stagnation-point flows

In section 2.3 we examined steady stagnation-point flows on an infinite flat plate in different situations, as a model for the flow in the neighbourhood of the stagnation point on a bluff body. Several authors have examined unsteady effects on such flows with a motivation, in part, prompted by aerodynamic flutter problems, and these we now consider.

4.7.1 Transverse oscillations

It is immaterial whether it is the plane boundary or oncoming stream which is oscillating. We assume the former, and that at large distances from the plane the steady two-dimensional flow represented by equation (2.32) is established. This problem has been considered both by Glauert (1956) and Rott (1956), with the boundary $y = 0$ oscillating in its own plane, with frequency ω and velocity amplitude U_0, in the x-direction. In place of (2.32) we now write

$$\psi = (\nu k)^{1/2} x f(\eta) + \left(\frac{\nu}{k}\right)^{1/2} U_0\, \mathrm{e}^{\mathrm{i}\omega t} \int_0^\eta g(\xi)\, \mathrm{d}\xi \quad \text{where again} \quad \eta = \left(\frac{k}{\nu}\right)^{1/2} y. \tag{4.60}$$

The pressure is given once more from equation (2.36), so that substitution of (4.60) into equation (1.9) gives

$$k^2 x(f''' + ff'' - f'^2 + 1) + kU_0\, \mathrm{e}^{\mathrm{i}\omega t} \left(g'' + fg' - f'g - \frac{\mathrm{i}\omega}{k} g\right) = 0,$$

from which we infer that f satisfies (2.35) and g satisfies

$$g'' + fg' - \left(f' + \frac{\mathrm{i}\omega}{k}\right) g = 0 \quad \text{with} \quad g(0) = 1, \quad g(\infty) = 0. \tag{4.61}$$

Solutions of equation (4.61) are sought by Glauert and Rott in the form of series, for example

$$g = \sum_{n=0}^{\infty} \left(\frac{\mathrm{i}\omega}{k}\right)^n g_n(\eta) \tag{4.62}$$

where the successive terms g_n are determined *seriatim*. The leading term $g_0(\eta)$ corresponds to the case when the plate slides in the x-direction with uniform speed, a case that has been considered in section 2.3. For large values of ω/k the representation (4.62) is not convenient and is replaced by

$$g = \sum_{n=0}^{\infty} \left(\frac{k}{\mathrm{i}\omega}\right)^{n/2} G_n(Y), \tag{4.63}$$

where we have $y = (\nu/\mathrm{i}\omega)^{1/2} Y$. The leading term now is $G_o = \mathrm{e}^{-Y}$ which is recognised as Stokes' solution (4.7), and indeed with subsequent terms of (4.63) containing a factor e^{-Y} the fluctuating flow is confined to the Stokes layer, thickness $O\{(\nu/\omega)^{1/2}\}$. The skin friction is given by

$$\mu \left.\frac{\partial u}{\partial y}\right|_{y=0} = (\rho\mu k)^{1/2} \{kxf''(0) + U_0\, \mathrm{e}^{\mathrm{i}\omega t} g'(0)\}.$$

In figure 4.8 we show $g'(0) = g_r'(0) + \mathrm{i}g_i'(0)$, and include results from the series (4.63).

By setting $\omega = -\mathrm{i}k$ Rott also considers the case in which the plate slides in the x-direction with speed $U_0\, \mathrm{e}^{kt}$, corresponding to a situation in which the plate accelerates from rest at $t = -\infty$. The solution of (4.61) for g is then, simply, $g = 1 - f'$. Rott also looks at the case when the time dependence is associated with motion in the z-direction. The basic steady stagnation-point

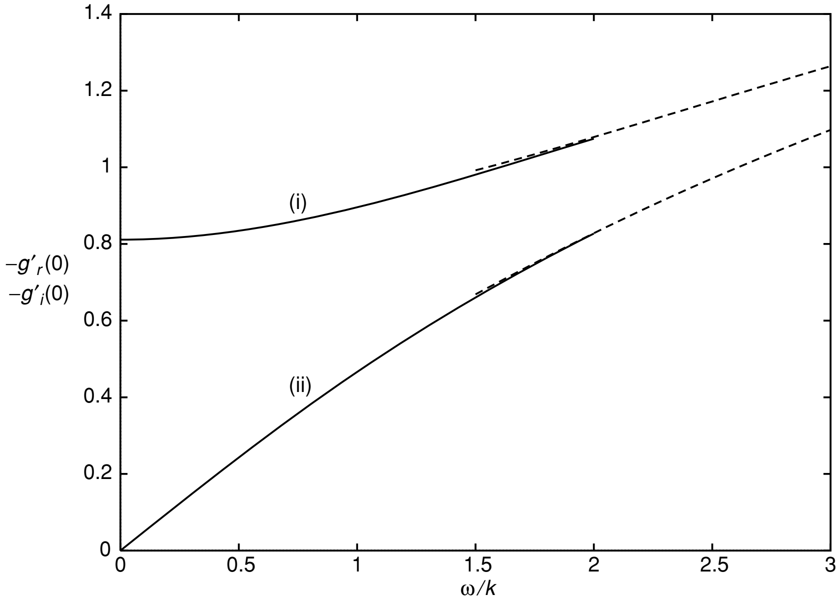

Figure 4.8 The shear stress contributions (i) $g_r'(0)$, (ii) $g_i'(0)$ at a transversely oscillating stagnation point; included in the figure are asymptotic results for $\omega/k \gg 1$, utilising seven terms of the series (4.63).

flow is represented by equation (2.32) with time dependence introduced by setting $w = W_0 h(\eta, \tau)$, with $\tau = kt$ and where h satisfies

$$h'' + fh' - \frac{\partial h}{\partial \tau} = 0, \quad \text{with} \quad h(0,\tau) = 1, \quad h(\infty,\tau) = 0. \tag{4.64}$$

The special case with $h \propto \mathrm{e}^{\mathrm{i}\tau}$ has been discussed in detail by Rott. Earlier, Wuest (1952), as well as considering more general cases, provided a numerical solution for one particular frequency.

As in section 4.3, Watson (1959) seeks to generalise these unsteady stagnation-point flows, using transform techniques, to accommodate more general plate motions. He writes, instead of (4.60),

$$\psi = (\nu k)^{1/2} x f(\eta) + \left(\frac{\nu}{k}\right)^{1/2} U_0 \int_0^\eta g(\xi,\tau)\,\mathrm{d}\xi \quad \text{with} \quad \eta \quad \text{as before and} \quad \tau = kt, \tag{4.65}$$

so that g now satisfies

$$g'' + fg' - f'g - \frac{\partial g}{\partial \tau} = 0 \quad \text{with} \quad g(0,\tau) = g_w(\tau) \quad \text{and} \quad g(\infty,\tau) = 0. \tag{4.66}$$

Supposing that the boundary is set into motion at $t = 0$, the Laplace transform

$$\tilde{g}(\eta, s) = \int_0^\infty e^{-s\tau} g(\eta, \tau)\, d\tau$$

is introduced, so that $\tilde{g}$ satisfies

$$\tilde{g}'' + f\tilde{g}' - f'\tilde{g} - s\tilde{g} = 0 \quad \text{with} \quad \tilde{g}(0, s) = \tilde{g}_w(s) \quad \text{and} \quad \tilde{g}(\infty, s) = 0. \tag{4.67}$$

It may be noted from (4.61) and (4.67) that the problem for $\tilde{g}/\tilde{g}_w$ is as that considered by Glauert and Rott when s replaces $i\omega/k$. Watson takes advantage of this by observing that the small-time solution, obtained by expanding $\tilde{g}/\tilde{g}_w$ for large s and inverting term by term can, in principle, be inferred from the series (4.63) and similarly the large-time solution obtained by expanding $\tilde{g}/\tilde{g}_w$ for small s from the series (4.62). In particular for the case of a boundary set into motion with uniform speed U_0 at time $t = 0$ Watson finds, for the skin friction,

$$\mu \frac{\partial u}{\partial y}\bigg|_{y=0} = (\rho\mu k)^{1/2} \left\{ kxf''(0) + U_0 \frac{\partial g}{\partial \eta}\bigg|_{\eta=0} \right\}$$

where, from the small-time result

$$\frac{\partial g}{\partial \eta}\bigg|_{\eta=0} = \frac{a_0}{(\pi\tau)^{1/2}} + 2a_1 \left(\frac{\tau}{\pi}\right)^{1/2} + \sum_{n=0}^{\infty} \frac{a_{n+3}\tau^{1+n/2}}{\Gamma(2 + \frac{1}{2}n)}, \tag{4.68}$$

where $a_i = dG_i/dY|_{Y=0}$ with $G_i(Y)$ as in (4.63). For large times the solution approaches the steady-state solution of Rott (1956) discussed in section 2.3 for which we have $\lim_{\tau\to\infty} \partial g/\partial\eta|_{\eta=0} = -0.8113$. In figure 4.9 $\partial g/\partial\eta|_{\eta=0}$ is shown, from the series (4.68), and this figure demonstrates how rapidly the steady state solution is reached following the impulsive start.

4.7.2 Orthogonal oscillations

In contrast to the flow in section 4.7.1 above we now consider the situation in which the steady stagnation-point flow is modified by the infinite plane performing harmonic fluctuations in its position along a normal direction. It is convenient, without loss of generality, to deal with the case in which the boundary is fixed with the far-field stagnation-point flow modulated by harmonic fluctuations of arbitrary amplitude and frequency. The study finds application to describe the local dynamics around a stagnation point on an oscillating body, or to model the local effects of disturbances at the stagnation point of a translating bluff body. The problem has received the attention of Grosch and Salwen (1982), Riley and Vasantha (1988), Merchant and Davis (1989) and Blyth and

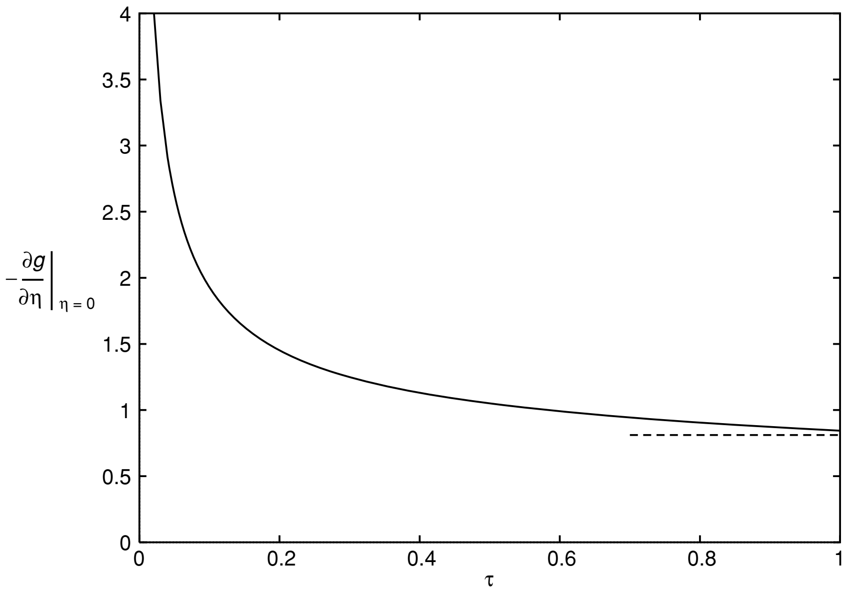

Figure 4.9 The shear stress contribution $\partial g/\partial\eta|_{\eta=0}$ calculated from six terms of the series (4.68).

Hall (2003), where the most recent of these investigations is the most comprehensive.

Far from the plane boundary $y = 0$ the modulated stagnation-point flow has the form

$$u = kx(1 + \Delta\cos\omega t), \quad v = -ky(1 + \Delta\cos\omega t),$$

and so we write, in place of (4.60),

$$\psi = (\nu k)^{1/2} x f(\eta, \tau) \quad \text{where} \quad \eta = \left(\frac{k}{\nu}\right)^{1/2} y \quad \text{and} \quad \tau = \omega t.$$

With the pressure now given by

$$\frac{p_0 - p}{\rho} = \frac{1}{2}k^2x^2a^2(\tau) + \frac{1}{2}\omega k x^2 a'(\tau) + \frac{1}{2}\nu k f^2 + \nu k f_\eta - \omega\nu\int_0^\eta f_\tau \, \mathrm{d}\eta, \tag{4.69}$$

$a(\tau) = 1 + \Delta\cos\tau$, equation (1.9) gives, for f,

$$\sigma f_{\eta\tau} = f_{\eta\eta\eta} + f f_{\eta\eta} - f_\eta^2 + \sigma a' + a^2, \tag{4.70}$$

together with

$$f(0, \tau) = f_\eta(0, \tau) = 0; \quad f_\eta(\infty, \tau) = a(\tau). \tag{4.71}$$

It may be noted that $\sigma = \omega/k$ is the Strouhal number.

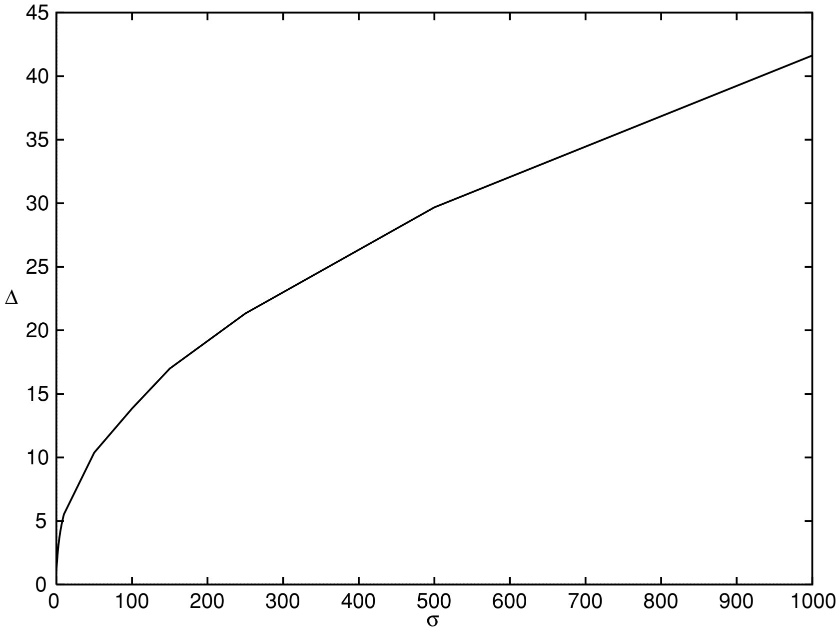

Figure 4.10 The 'barrier', calculated by Blyth and Hall (2003), above which the solution develops a singularity at a finite time.

Grosch and Salwen addressed the problem posed by equations (4.70) and (4.71) for small Δ by expanding the solution as Fourier series in τ with coefficients functions of η, each expanded in powers of Δ. For $\sigma \ll 1$ the solution is a quasi-steady version of the classical Hiemenz solution. For $\sigma \gg 1$ the solution exhibits a double structure. Merchant and Davis take advantage of this double structure for large σ to develop solutions of (4.70), (4.71) when $\Delta \gg 1$. A steady streaming is induced due to the action of Reynolds stresses within the inner Stokes shear-wave layer, thickness $O\{(\nu/\omega)^{1/2}\}$, which persists beyond it, where it is determined as the solution of an ordinary differential equation. Merchant and Davis show that this equation has no solution when $\Delta > 1.289\sigma^{1/2}$.

Blyth and Hall have set these earlier results into a wider context by integrating the differential equation (4.70) forward in time starting from a state of rest. They show that for each value of σ the solution develops a singularity at a finite time for Δ sufficiently large. From their extensive calculations they are able to determine the critical curve in (σ, Δ) parameter space that delineates the regular periodic solutions from those which blow up in a finite time, τ_s, and this result is shown in figure 4.10. In particular as $\sigma \to \infty$ they are able to refine the result of Merchant and Davis, and find $\Delta \sim 1.289\sigma^{1/2} + 0.76$ which

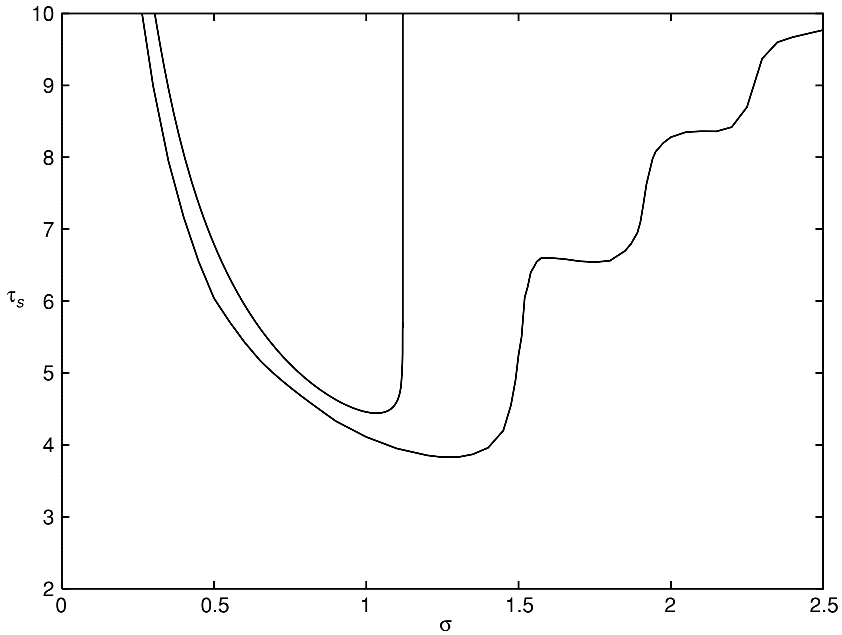

Figure 4.11 Examples showing the 'blow-up' time for $\Delta = 2.0$, Blyth and Hall (2003), and Δ indefinitely large, Riley and Vasantha (1988). In the former case the barrier of figure 4.10 is encountered at $\sigma \approx 1.12$ beyond which the solution is regular.

is almost indistinguishable from the result shown in figure 4.10 for $\sigma > 20$. As $\sigma \to 0$ the critical value of $\Delta \to 1+$. This is a singular limit since for $\sigma \equiv 0$ the steady Hiemenz solution is recovered. The result as $\sigma \to 0$ shows that only the smallest amount of flow reversal in the onset flow is required to initiate a catastrophic failure of the solution.

Riley and Vasantha (1988) were concerned with the case in which the onset flow has zero mean, which in the present context corresponds, formally, to $\Delta \to \infty$. Their results, consistent with those described above, show a breakdown of the solution at a finite time for all non-zero values of σ. In figure 4.11 we compare the breakdown time determined by Blyth and Hall for $\Delta = 2$ with that of Riley and Vasantha.

The failure, or blow-up, of the solution at a finite time is not localised in space but occurs over the entire flow domain with the velocity components $u \propto (\tau_s - \tau)^{-3/2}$, $v \propto (\tau_s - \tau)^{-1}$. In this sense it differs from the problem of blow-up identified by Leray (1934), in which velocities scale with $(\tau_s - \tau)^{-1/2}$ and the singularity is located at a point about which length scales decrease as $(\tau_s - \tau)^{1/2}$. However, in common with Leray the solution discussed here does not have finite total energy, and caution must be exercised before any conclusions are reached about the adequacy, or otherwise, of the Navier–Stokes equations as a mathematical model for incompressible fluid flow in any realistic situation. Vasantha and Riley interpret the singular behaviour as $\tau \to \tau_s-$ as a disruptive event in which a net drift of fluid particles towards the stagnation point leads to an accumulation and consequent eruption of fluid from the stagnation point. In a different, but not dissimilar, situation experiments by Wybrow and Riley (1995) visualise such an eruption as a jet headed by a vortex pair.

4.7.3 Superposed shear flows

The stagnation-point flow, with $\mathbf{v} = (cx, -cy, 0)$, is an exact solution of the Navier–Stokes equations but it cannot satisfy all the usual conditions at any solid boundary. However, in an unbounded region the stresses are everwhere continuous, and the exact solution represents the impingement of two stagnation-point flows, in $y > 0$ and $y < 0$, at the interface $y = 0$. Kambe (1983) superposes on this a shear flow in the x-direction, and simultaneously modulates the basic flow with time by writing

$$u = \frac{\mathrm{d}k}{\mathrm{d}t}x - F(y, t), \qquad v = -\frac{\mathrm{d}k}{\mathrm{d}t}y,$$

where $k = k(t)$. The only non-zero component of vorticity is in the z-direction and has $\zeta = \partial F/\partial y$. From equations (1.13) and (1.16) it satisfies the equation

$$\frac{\partial \zeta}{\partial t} - \frac{\mathrm{d}k}{\mathrm{d}t}y\frac{\partial \zeta}{\partial y} = \nu\frac{\partial^2 \zeta}{\partial y^2}. \tag{4.72}$$

By writing $\eta = \mathrm{e}^k y$ and $\tau = \int_0^t \mathrm{e}^{2k}\,\mathrm{d}t$, the vorticity transport equation (4.72) transforms to

$$\frac{\partial \zeta}{\partial \tau} = \nu\frac{\partial^2 \zeta}{\partial \eta^2}. \tag{4.73}$$

If we assume $k(0) = 0$, then an initial distribution of vorticity $\zeta(y, 0) = \zeta_0(y) = \zeta_0(\eta)$ leads to a solution of equation (4.73), analogous to that discussed in section 4.2.3, as

$$\zeta(\eta, \tau) = \frac{1}{2}(\pi\nu\tau)^{1/2}\int_{-\infty}^{\infty}\zeta_0(s)\exp\left\{-\frac{(s-\eta)^2}{4\nu\tau}\right\}\mathrm{d}s. \tag{4.74}$$

As one example Kambe considers a vortex sheet along the interface $y = 0$ at the initial instant such that

$$F(y, 0) = \begin{cases} U_0, & y > 0, \\ -U_0, & y < 0. \end{cases}$$

This is consistent with $\zeta_0(y) = 2U_0\delta(y)$, where δ is the Dirac delta function. The solution (4.74) is then the Gaussian shear layer

$$\zeta(\eta, \tau) = \frac{U_0}{(\pi\nu\tau)^{1/2}} \mathrm{e}^{-(y/a)^2} \quad \text{where} \quad a = 2(\nu\tau)^{1/2}\mathrm{e}^{-k}. \tag{4.75}$$

With $\partial F/\partial y = \zeta$ we have, for the velocity field,

$$u = \frac{\mathrm{d}k}{\mathrm{d}t}x - U_0\,\mathrm{e}^{-a}\mathrm{erf}(y/a), \quad v = -\frac{\mathrm{d}k}{\mathrm{d}t}y.$$

For the special case $\mathrm{d}k/\mathrm{d}t = \text{constant} = c > 0$, $k = ct$ and $\tau = (\mathrm{e}^{2ct} - 1)/2c$ so that, as $t \to \infty$, we have from (4.75)

$$\zeta \sim \left(\frac{2c}{\pi\nu}\right)^{1/2} U_0\,\mathrm{e}^{-ct}\,\mathrm{e}^{-cy^2/2\nu}$$

which implies that, in the final stages, there is a region of vorticity of unchanging shape which decays exponentially with time.

Other examples analysed by Kambe include the case of two vortex sheets which form, initially, a 'top hat' jet for $|y| < y_0$ and the situation in which at the initial instant the distribution of vorticity is represented by two Gaussian distributions centred on $y = -y_0$ and $y = y_0$. Kambe (1986) has also generalised these ideas to three-dimensional situations.

4.7.4 Three-dimensional stagnation-point flow

As in section 2.5.4 we introduce a three-dimensional stagnation-point flow which, as in the steady case, embraces both the two-dimensional and axisymmetric flows. Such a flow has been considered by Cheng, Özişik and Williams (1971). As for the steady case it is convenient to adopt a slight change of notation with x, y as co-ordinates in the plane and z perpendicular to it. Cheng *et al.* assume that far from the boundary the x and y components of velocity are given by $u = kx/(1 + \alpha\omega t)$, $\quad v = ly/(1 + \alpha\omega t)$ where k, l, α and ω are constants, and introduce a self-similar solution as

$$u = \frac{kx}{1 + \alpha\tau} f'(\eta), \quad v = \frac{ky}{1 + \alpha\tau} g'(\eta), \quad w = -\left(\frac{\nu k}{1 + \alpha\tau}\right)^{1/2} \{f(\eta) + g(\eta)\}, \tag{4.76}$$

where

$$\eta = \left\{ \frac{k}{\nu(1+\alpha\tau)} \right\}^{1/2} z \quad \text{and} \quad \tau = \omega t.$$

With $r = l/k$ and $\sigma = \alpha\omega/k$, introducing (4.76) into equations (1.9) to (1.11) yields the equations for f and g as

$$f''' + (f+g)f'' - f'^2 + 1 + \sigma\left(f' + \tfrac{1}{2}\eta f'' - 1\right) = 0$$
$$\text{with} \quad f(0) = f'(0) = 0, \quad f'(\infty) = 1,$$

$$g''' + (f+g)g'' - g'^2 + r^2 + \sigma\left(g' + \tfrac{1}{2}\eta g'' - r\right) = 0$$
$$\text{with} \quad g(0) = g'(0) = 0, \quad g'(\infty) = r,$$

and the pressure as

$$\frac{p_0 - p}{\rho} = \frac{1}{2(1+\alpha\tau)^2}\{k^2(1-\sigma)x^2 + l^2(1-\sigma)y^2 + \frac{k\nu}{2(1+\alpha\tau)}\{2(f'+g') + (f+g)^2 + \sigma\eta(f+g)\}.$$

Numerical solutions of the equations for f and g are presented by Cheng *et al.* for a range of values of r and σ, although the analogues of the dual solutions of Davey and Schofield (1967) and Schofield and Davey (1967) do not appear to have been explored.

As for the steady case, values of $r > 0$ and $r < 0$ correspond, respectively, to nodal and saddle points of attachment; values of $\alpha > 0$ and $\alpha < 0$ correspond to decelerating and accelerating flows respectively. In common with other self-similar solutions it is not possible to prescribe the velocity profiles (u, v) at some initial instant $t = 0$. Accepting they are given by (4.76) then, for $\alpha > 0$, the flow decays, in a region that increases in thickness $\propto (1+\alpha\tau)^{1/2}$. By contrast, for $\alpha < 0$ the flow accelerates, in a region of diminishing thickness, and terminates in a singularity at time $t = t_s = (\alpha\omega)^{-1}$. Unlike the situation discussed in the previous section, where the singular behaviour develops spontaneously, the singular behaviour is built in to the solution (4.76).

For $\sigma = 0$ the solution (4.76) coincides with the steady solution (2.77), whilst for $r = 0$ the two-dimensional unsteady solution, first considered by Yang (1958), is recovered. The case $r = 0$, and the axisymmetric flow case $r = 1$, have been considered by Williams (1968). Yang in particular shows that as σ increases, that is as the deceleration rate increases, a value is reached, namely $\sigma = 3.1625$, at which $f''(0) = 0$; for higher deceleration rates there is

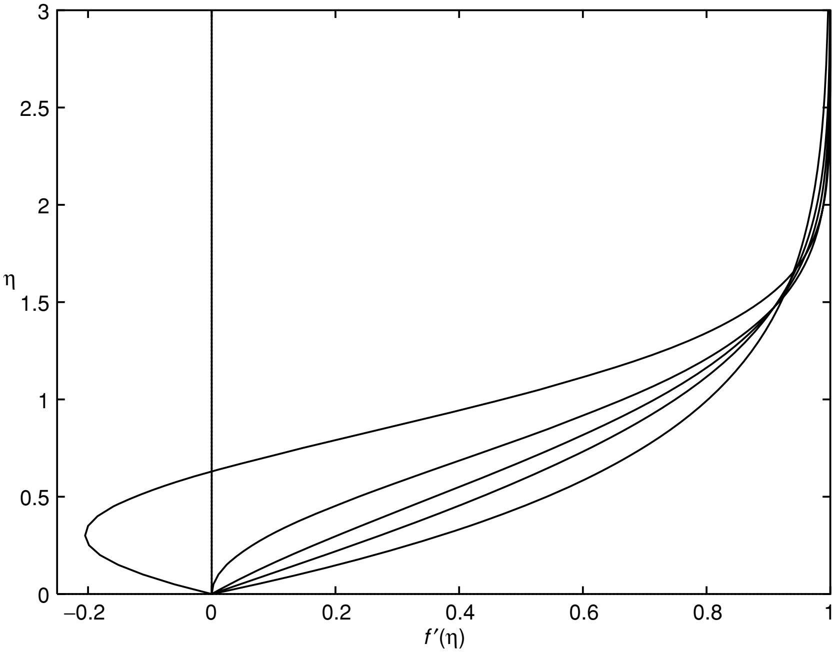

Figure 4.12 Velocity profiles $f'(\eta)$, for the two-dimensional flow corresponding to $r = 0$, for $\sigma = 4.5$ (uppermost), 3.1625, 2.0, 1.0, -1.0.

a region of reversed flow close to the boundary. The corresponding value for $r = 1$ is given by Cheng *et al.* as $\sigma = 3.7173$, at which $f''(0) = g''(0) = 0$. From their results Cheng *et al.* note that for $|\sigma| < 1$ and $0 < r < 1$ the velocity profiles $f'(\eta)$, $g'(\eta)$ differ little from the corresponding steady state profiles. Rajappa (1979) extended Yang's solution to include the effects of hard blowing from the boundary.

In figure 4.12 we show representative velocity profiles for the case of two-dimensional flow $r = 0$.

4.7.5 Rotational three-dimensional stagnation-point flow

Hersh (1970) considers a stagnation-point flow in which there is an unsteady element of lateral vorticity. He takes

$$\mathbf{v} = k\{F(z,t) + (1-\alpha_0)x, -G(z,t) + (1+\alpha_0)y, -2z\}, \quad 0 \le \alpha_0 < 1, \tag{4.77}$$

for which the corresponding vorticity field is given by $\boldsymbol{\omega} = k(\partial G/\partial z, \partial F/\partial z, 0)$. A self-similar solution is obtained for $\boldsymbol{\omega}$ by writing, for the x-component,

$$k\frac{\partial G}{\partial z} = g(\tau)f(\eta) \quad \text{where} \quad \tau = kt \quad \text{and} \quad \eta = \left(\frac{k}{\nu}\right)^{1/2} h(\tau)z. \tag{4.78}$$

Introducing (4.77) and (4.78) into the vorticity transport equation (1.16) gives

$$\frac{\mathrm{d}^2 f}{\mathrm{d}\eta^2} + \left(\frac{2h - \mathrm{d}h/\mathrm{d}\tau}{h^3}\right)\eta\frac{\mathrm{d}f}{\mathrm{d}\eta} + \left\{\frac{(1-\alpha_0)g - \mathrm{d}g/\mathrm{d}\tau}{gh^2}\right\} f = 0. \tag{4.79}$$

Equation (4.79) is satisfied provided that

$$h(\tau) = (1 + a\,\mathrm{e}^{-4\tau})^{-1/2}, \quad g(\tau) = (1 + a\,\mathrm{e}^{-4\tau})^{(\alpha_0 - 1)/4}, \tag{4.80}$$

where a is an arbitrary constant and, with $\xi = -\eta^2$, f satisfies the confluent hypergeometric equation

$$\xi\frac{\mathrm{d}^2 f}{\mathrm{d}\xi^2} + \left(\frac{1}{2} - \xi\right)\frac{\mathrm{d}f}{\mathrm{d}\xi} - \frac{(1-\alpha_0)}{4}f = 0.$$

Finally then, from (4.80) and (4.78), the x-component of vorticity is given by

$$\begin{aligned} k\frac{\partial G}{\partial z} &= (1 + a\,\mathrm{e}^{-4kt})^{(\alpha_0 - 1)/4} \exp\left\{-\frac{kz^2}{\nu(1 + a\,\mathrm{e}^{-4kt})}\right\} \\ &\times \left\{A\,{}_1F_1\left(\frac{1+\alpha_0}{4}; \frac{1}{2}; \frac{kz^2}{\nu(1 + a\,\mathrm{e}^{-4kt})}\right) + B\frac{(k/\nu)^{1/2}z}{(1 + a\,\mathrm{e}^{-4kt})^{1/2}}\right. \\ &\left.\times\, {}_1F_1\left(\frac{3+\alpha_0}{4}; \frac{3}{2}; \frac{kz^2}{\nu(1 + a\,\mathrm{e}^{-4kt})}\right)\right\}, \end{aligned} \tag{4.81}$$

where A and B are arbitrary constants. The solution for the y-component of vorticity $k\partial F/\partial z$ follows in a similar manner; the result is as in equation (4.81) with the sign of α_0 changed.

The solution so obtained, with the velocity field following from integration with respect to z, is an exact solution of the vorticity transport equation, but is of limited value. For example, for no choice of A and B can the no-slip condition be satisfied; and the velocity field will only be bounded, as $z \to \infty$, if

$$\frac{A}{B} = -\frac{\Gamma\left(\frac{\alpha_0+1}{4}\right)}{2\Gamma\left(\frac{\alpha_0+3}{4}\right)}.$$

However, the plane $z = 0$ can only represent the interface between two opposing streams if $A \equiv 0$, otherwise the shear stress is discontinuous there.

4.7.6 Flow at a rear stagnation point

In section 2.3 we considered the classical two-dimensional steady stagnation-point flow on the plane boundary $y = 0$ due to Hiemenz (1911). This was proposed as the flow that prevails at the front stagnation point of a blunt cylindrical body in steady flow. At a rear stagnation point, on a circular cylinder say, the situation is different. Common observation shows that following an impulsive start when the flow is everywhere irrotational, with the exception of a vortex sheet at the surface, reversed flow develops as the region of vortical flow thickens rapidly. In contrast with the front stagnation point, where a balance is achieved between diffusion of vorticity and the inhibiting onset flow resulting in a steady state, diffusion of vorticity is reinforced by advection to ensure that no steady state is possible. Proudman and Johnson (1962) model this by considering a 'rear' stagnation-point flow on a plane boundary. For an inviscid fluid the appropriate irrotational flow is simply $u = -kx, \quad v = ky$. For a viscous fluid it is then natural to write, instead of (2.32),

$$\psi = -(\nu k)^{1/2} x f(\eta, \tau) \quad \text{where} \quad \tau = kt \quad \text{and} \quad \eta = \left(\frac{k}{\nu}\right)^{1/2} y, \tag{4.82}$$

and for the pressure, instead of (2.36), we have

$$\frac{p_0 - p}{\rho} = \frac{1}{2}k^2x^2 + \nu k\left(\frac{1}{2}f^2 + f_\eta + \int_0^\eta f_\tau \, \mathrm{d}\eta\right).$$

Equation (1.9) then gives, for $f(\eta, \tau)$,

$$\begin{aligned} &f_{\eta\tau} - f_\eta^2 + f f_{\eta\eta} - f_{\eta\eta\eta} = -1, \\ &\text{with} \quad f(0, \tau) = f_\eta(0, \tau) = 0, \quad f_\eta(\infty, \tau) = 1. \end{aligned} \tag{4.83}$$

Equation (4.83) may be compared with (2.35). In particular it should be noted that if a steady state is assumed such that $f_{\eta\tau} \equiv 0$, the resulting equation has no solution.

Proudman and Johnson attack equation (4.83) by a variety of analytical and numerical methods, with the vortex sheet at the surface as an initial state. Their investigation has been extended by Robins and Howarth (1972). Principal amongst the results obtained are (a) that flow reversal first takes place close to $y = 0$ at $\tau \approx 0.65$, and that thereafter the flow divides into a wall region of reversed flow and an outer region of forward flow as required by the condition at infinity in (4.83), and (b) that as $\tau \to \infty$ the vortical layer thickness $\delta_v = O\{(\nu/k)^{1/2}\,\mathrm{e}^\tau\}$. This latter result demonstrates that the dynamics of the flow close to the rear stagnation point with its flow reversal must not be confused with onset of boundary-layer separation. At any finite time, as $\nu \to 0$, $\delta_v \to 0$, whereas boundary-layer separation is associated with an unbounded δ_v at a finite time as $\nu \to 0$. The apparent paradox was resolved by van Dommelen and Shen (1980). Their investigation shows that for a circular cylinder the solution of the boundary-layer equations breaks down at a finite time, namely $\tau_s \approx 1.5$, away from the rear stagnation point.

4.8 Channel flows

As for steady flows, unsteady flow in parallel-sided channels has attracted attention with and without transpiration at the two boundaries. Such investigations may find application in the modelling of haemodialysis, pulsating diaphragms, transpiration cooling, isotope separation and filtration. An obvious source of unsteadiness is a time-dependent pressure gradient, but unsteadiness due to movement of the bounding channel walls either in their own planes, or more interestingly normal to them, is also possible.

4.8.1 Fixed boundaries

Wang (1971) has considered the case of a channel with fixed, but porous, walls distance h apart, across which fluid is drawn with uniform speed V and between which there is a fluctuating pressure gradient

$$\frac{1}{\rho}\frac{\partial p}{\partial x} = P_1 + P_2 \cos \omega t.$$

With $\mathbf{v} = \{u(y, t), V, 0\}$ the x-component of velocity may be separated into a time-dependent and time-independent part by writing $u(y, t) = u_1(y) + u_2(y)\,\mathrm{e}^{i\omega t}$, where the real part is to be understood. The solution for u_1 is determined, from equation (2.3), as

$$\frac{u_1}{P_1 h/V} = \frac{\mathrm{e}^{R\eta} - 1}{\mathrm{e}^{R} - 1} - \eta,$$

where $R = Vh/\nu$ and $\eta = y/h$. For the time-dependent part of u, which from equation (1.9) satisfies

$$\frac{\partial u_2}{\partial t} + V\frac{\partial u_2}{\partial y} = -P_2\mathrm{e}^{\mathrm{i}\omega t} + \nu\frac{\partial^2 u_2}{\partial y^2}, \tag{4.84}$$

we may write $u_2(y, t) = (P_2 h^2/\nu) f(\eta)\,\mathrm{e}^{\mathrm{i}\omega t}$, so that from (4.84) f satisfies

$$f'' - Rf' - \mathrm{i}M^2 f = 1, \quad \text{where} \quad M^2 = \omega h^2/\nu. \tag{4.85}$$

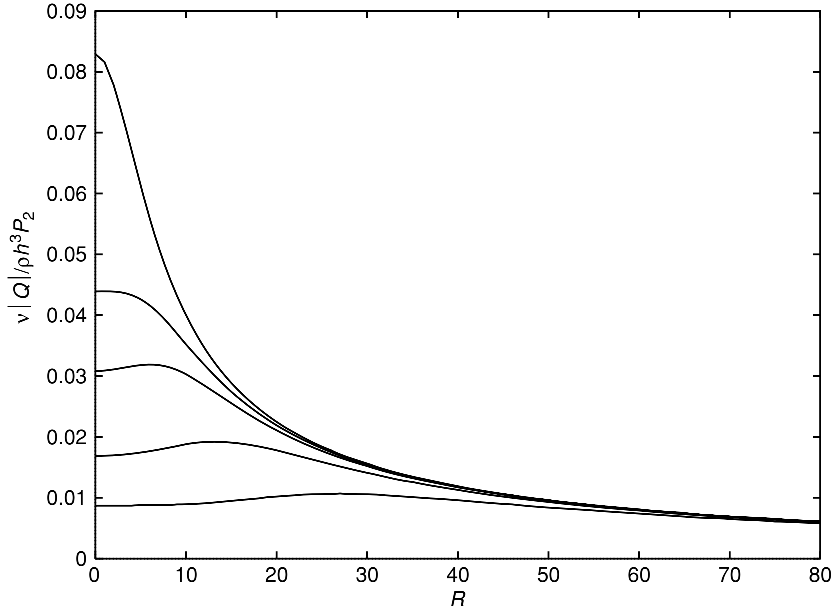

Figure 4.13 The magnitude of the instantaneous mass flux along the channel for cases $M = 1$ (uppermost), 4, 5, 7, 10.

And with $f(0) = f(1) = 0$, the required solution of equation (4.85) is

$$\frac{u_2}{P_2 h^2/\nu} = \frac{\mathrm{i}}{M^2}\left\{1 + \frac{(1 - \mathrm{e}^{\lambda_2})\mathrm{e}^{\lambda_1 \eta} - (1 - \mathrm{e}^{\lambda_1})\,\mathrm{e}^{\lambda_2 \eta}}{\mathrm{e}^{\lambda_2} - \mathrm{e}^{\lambda_1}}\right\}\mathrm{e}^{\mathrm{i}\omega t}, \tag{4.86}$$

with

$$\lambda_{1,2} = \frac{R \pm (R^2 + 4\mathrm{i}M^2)^{1/2}}{2}.$$

For small R both u_1 and u_2 are essentially symmetric about the channel centre-line $y = h/2$, regardless of the value of M. As R increases both exhibit a degree of asymmetry which is reflected in the mass flux along the channel. The instantaneous mass flux Q is given by, using (4.86),

$$\frac{Q}{\rho h^3 P_2/\nu} = \frac{\mathrm{i}\,\mathrm{e}^{\mathrm{i}\omega t}}{M^2}\left\{1 + \frac{(\mathrm{e}^{\lambda_1} - 1)(\mathrm{e}^{\lambda_2} - 1)(\lambda_1 - \lambda_2)}{\lambda_1 \lambda_2 (\mathrm{e}^{\lambda_2} - \mathrm{e}^{\lambda_1})}\right\},$$

whose magnitude is shown as a function of R in figure 4.13 for various values of M.

4.8.2 Squeeze flows

The squeezing of a fluid between two plates may be considered as a model for the unsteady loading of mechanical parts as, for example, in thrust bearings. For such a configuration the stagnation-point flow considered in section 4.7.4 suggests a self-similar form of solution in which for plates situated at $y = y_p = \pm h(t)$ we have $h(t) = h_0(1-\alpha t)^{1/2}$. This is the approach adopted by Wang (1976) who takes

$$\psi = \frac{\alpha h_0 x}{2(1-\alpha t)^{1/2}} f(\eta) \quad \text{where} \quad \eta = \frac{y}{h} = \frac{y}{h_0(1-\alpha t)^{1/2}},$$

so that

$$u = \frac{\alpha x}{2(1-\alpha t)} f'(\eta) \quad \text{and} \quad v = -\frac{\alpha h_0}{2(1-\alpha t)^{1/2}} f(\eta), \tag{4.87}$$

and the equation for $f(\eta)$ is, from (1.9),

$$\frac{2\,\mathrm{sgn}\,\alpha}{M^2} f''' + ff'' - f'^2 - \eta f'' - 2f' = A, \tag{4.88}$$

where $M^2 = |\alpha| h_0^2/\nu$ and A is a constant. Since the flow is symmetrical about $y = 0$ equation (4.88) is to be solved subject to the boundary conditions

$$f(0) = f''(0) = 0; \quad f(1) = 1, \quad f'(1) = 0, \tag{4.89}$$

and the constant A then takes the value $A = 2\,\mathrm{sgn}\,\alpha f'''(1)/M^2$, which is not determined *a priori*. The pressure is now given by

$$\frac{p_0 - p}{\rho} = -\frac{A\alpha^2 x^2}{8(1-\alpha t)^2} + \frac{\alpha^2 h_0^2}{8(1-\alpha t)} \left(f^2 - 2\eta f + \frac{4\,\mathrm{sgn}\,\alpha}{M^2} f' \right),$$

where p_0 may now be a function of t.

For $\alpha > 0$ the plates draw together and touch at $t = \alpha^{-1}$, when all other flow variables become unbounded. The velocity profiles $f'(\eta)$ for this case are shown in figure 4.14. As M increases , boundary layers develop adjacent to the plates, and the bulk of the fluid is squeezed out with uniform velocity. For $\alpha < 0$ the plates are drawn apart and, depending upon the value of M, the profiles exhibit different characteristics as shown in figure 4.15. For sufficiently small M fluid is drawn inwards at all points in the gap; but as M increases we see that an outflow develops in the neighbourhood of the boundaries.

There is a qualitative similarity between the velocity profiles shown in figures 4.14 and 4.15 and the steady state situation in which fluid is injected or withdrawn across the fixed porous boundaries of a channel as discussed in chapter 2. In particular, boundary layers form as M increases when the plates are squeezed together, whilst as they are drawn apart a region of reversed flow develops as M increases.

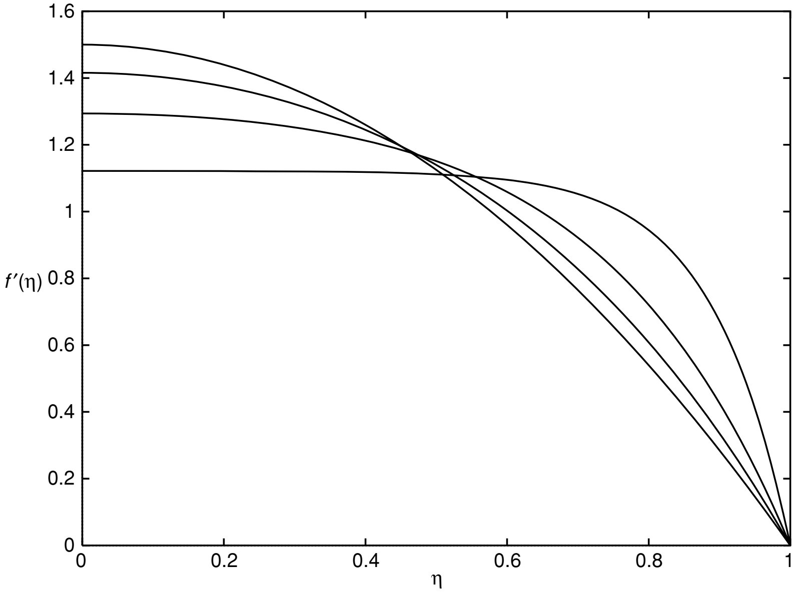

Figure 4.14 Velocity profiles $f'(\eta)$ for squeeze flows corresponding to $\alpha > 0$ with $M = 0.0$ (uppermost), 1.498, 2.879, 7.204.

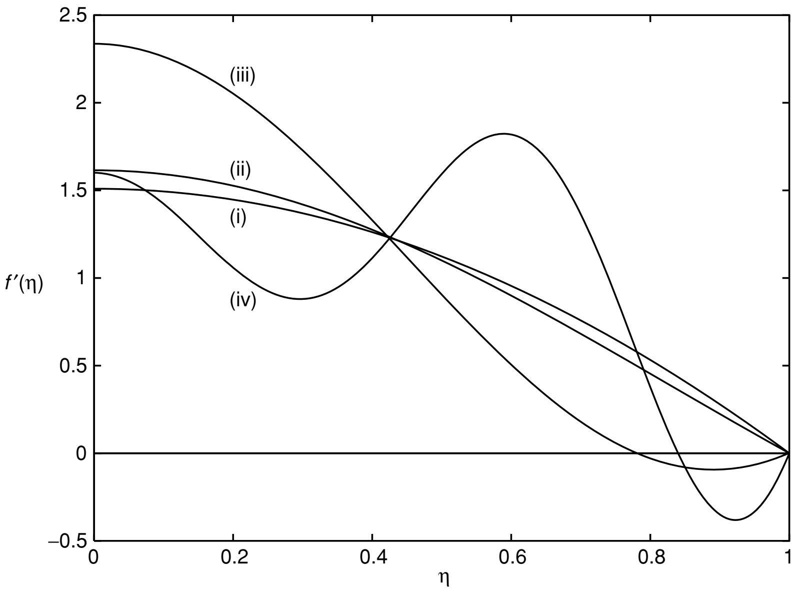

Figure 4.15 Velocity profiles $f'(\eta)$ for squeeze flows corresponding to $\alpha < 0$ with (i) $M = 0.447$, (ii) 1.399, (iii) 2.2214, (iv) 7.195.

Dauenhauer and Majdalani (2003) have extended the range of solutions of equation (4.88) by allowing transpiration across the moving boundaries at $y = \pm h$. The boundary condition on f at $\eta = 1$ in (4.89) is modified to accommodate this. Results are presented for various injection/suction rates with the boundaries closing together or moving apart.

The possibility of multiple solutions, a feature of the steady flow between porous boundaries discussed in section 2.4.1, does not appear to have been addressed in either of the above investigations.

In an earlier paper Thorpe (1967) considered the general case in which the plates are in position $y_p = \pm h(t)$. By writing

$$u = -\frac{1}{h}\frac{\mathrm{d}h}{\mathrm{d}t} x f'(\eta), \quad v = \frac{\mathrm{d}h}{\mathrm{d}t} f(\eta) \quad \text{where} \quad \eta = \frac{y}{h}, \tag{4.90}$$

Thorpe shows from equation (1.9) that $\partial p/\partial\eta$ is again independent of x, so that $\partial^2 p/\partial\eta\partial x = 0$. Differentiating (1.9) with respect to y, and u, v as in (4.90) gives

$$\frac{h}{\nu}\frac{\mathrm{d}h}{\mathrm{d}t}(2f'' + \eta f''' + f'f'' - ff''') + f^{iv} = \frac{h^2}{\nu \mathrm{d}h/\mathrm{d}t}\frac{\mathrm{d}^2 h}{\mathrm{d}t^2} f''. \tag{4.91}$$

At this stage the similarity-solution procedure would seek to ensure that the coefficients of the bracketed expression on the left-hand side of equation (4.91) and of f'' on its right-hand side are constant. Such a procedure leads directly to the form of solution in equation (4.87). However, Thorpe noted that if

$$f = \eta + \frac{(-1)^{n+1}}{n\pi}\sin n\pi\eta, \tag{4.92}$$

then equation (4.91) will be satisfied provided that $h(t)$ satisfies the non-linear equation

$$\frac{\mathrm{d}^2 h}{\mathrm{d}t^2} + (n\pi)^2\frac{\nu}{h^2}\frac{\mathrm{d}h}{\mathrm{d}t} - \frac{3}{h}\left(\frac{\mathrm{d}h}{\mathrm{d}t}\right)^2 = 0.$$

A detailed study of this equation does not appear to have been carried out. However, one solution is readily shown to be $h = h_0(1 - \alpha t)^{1/2}$ where $\alpha = -(n\pi)^2\nu/2h_0^2$ which then leads to (4.87), where f satisfies equation (4.88) with $M^2 = (n\pi)^2/2$, whose solution is given by (4.92). This case is included in figure 4.15 with $M = \pi/\sqrt{2} = 2.2214$ corresponding to $n = 1$, and is characterised by the vanishing of f'' at $\eta = 1$.

Hall and Papageorgiu (1999) have considered the case when $h(t)$ is a prescribed periodic function of time. They demonstrate that the flow may break down chaotically following an instability associated with the time dependence. The amplitude of the oscillation that the squeeze flow can support before breakdown is determined; and it is noted that load bearing properties may change significantly when breadown occurs.

4.8.3 Periodic solutions

Watson, Banks, Zaturska and Drazin (1991) and Cox (1991b) have reconsidered the steady channel flows of section 2.4.1, in particular for asymmetric flows. The former achieve this by allowing the boundaries to stretch, that is $u \propto x$ at $y = \pm h$, at different rates, whilst Cox, with both boundaries fixed, has transpiration across one with the other impermeable. In both of these situations it is shown that time-periodic limit-cycle solutions emerge following Hopf bifurcations.

Wave-like flows have been considered by Hui (1987) as follows. With $\alpha = -K$ and with U constant equations (4.52) and (4.53) become

$$\nabla^2\psi = K(\psi - Uy) \quad \text{and} \quad \frac{\partial\psi}{\partial t} + U\frac{\partial\psi}{\partial x} = \nu\nabla^2\psi \quad \text{respectively.}$$

Then, letting $\Psi = \psi - Uy$ in the above gives

$$\nabla^2\Psi = K\Psi \quad \text{and} \quad \frac{\partial\Psi}{\partial t} + U\frac{\partial\Psi}{\partial x} = \nu K\Psi. \tag{4.93}$$

The second of equations (4.93) is satisfied identically by $\Psi = \mathrm{e}^{\nu Kt}F(X, y)$ where $X = x - Ut$; letting $F(X, y) = f(\xi)$ where $\xi = X\cos\beta + y\sin\beta$, with β constant, the first of (4.93) becomes $f'' - Kf = 0$. With $K = -k^2$, for example, $f(\xi) = A\cos\{k(\xi + B)\}$ for constant A, B so that, finally,

$$\psi = Uy + A\,\mathrm{e}^{-\nu k^2 t}\cos\{k(x\cos\beta + y\sin\beta - Ut\cos\beta)\} \tag{4.94}$$

which represents a decaying, travelling, periodic wave superposed on a uniform stream. This plane wave, wavenumber k, propagates with speed $U\cos\beta$ at an angle β to the x-axis. It may be noted that since $U\cos\beta$ is the component of the free-stream velocity in a direction normal to the wave fronts, signals are carried by the undisturbed uniform flow. Streamline patterns from (4.94), at different values of t, are shown in figure 4.16.

Hui discusses another class of solutions by writing $\Psi = \mathrm{e}^{\nu Kx/U}g(\xi)$, with ξ as before. Again the second of equations (4.93) is satisfied identically whilst the first now requires

$$g'' + \frac{2\nu K}{U}\cos\beta g' + K\left(\frac{\nu^2 K}{U^2} - 1\right)g = 0,$$

so that with $g \propto \mathrm{e}^{\lambda\xi/U}$ we have the two possibilities for λ, namely

$$\lambda_{1,2} = -\nu K\cos\beta \pm K\nu\left(\frac{U^2}{K\nu^2} - \sin^2\beta\right)^{1/2}.$$

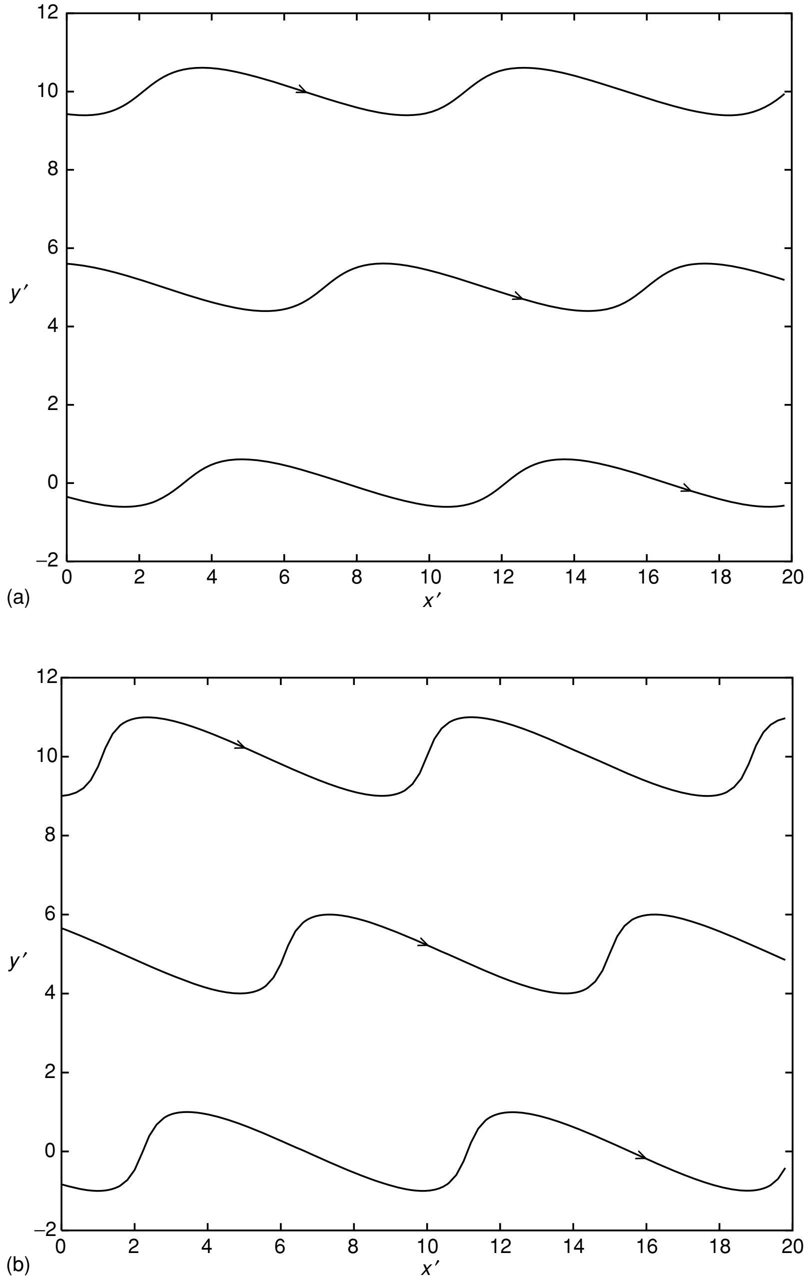

Figure 4.16 Streamline patterns for the wave superposed on a uniform stream, equation (4.94). In these illustrations the variables are dimensionless such that in (4.94) a typical length is taken as k^{-1}, time $(kU)^{-1}$ and a stream function U/k. Values $\beta = \pi/4$, $\quad Ak/U = 1$ and $R = U/\nu k = 2$ have been chosen. For the streamlines $\psi' = 10$ (uppermost), 5, 0. (a) $t' = 0$. (b) $t' = 1$.

An example, with $K = -k^2$ gives

$$\psi = Uy + \exp\left\{-\frac{\nu k^2}{U}\left(x\sin^2\beta - \frac{1}{2}y\sin 2\beta + Ut\cos^2\beta\right)\right\}$$
$$\times \cos[k\{1 + (\nu k/U)^2\sin^2\beta\}^{1/2}\{x\cos\beta + y\sin\beta - Ut\cos\beta\}],$$

which again represents a periodic travelling wave whose amplitude now varies both spatially and temporally.

Results similar to those obtained by Hui may be inferred from the papers by Grauel and Steeb (1985) and Moore (1991).

Craik and Criminale (1986) also superpose disturbances on basic shear flows, which may be two- or three-dimensional possessing spatially uniform, but not necessarily steady, strain rates so that

$$\mathbf{V} = \mathbf{S}\mathbf{x} + \mathbf{V}_0(t) \quad \text{where} \quad \mathbf{S} \equiv \{\sigma_{ij}(t)\}.$$

The disturbance is denoted by $\mathbf{v}'$ so that $\mathbf{v} = \mathbf{V} + \mathbf{v}'$. Since the 'disturbance' may have arbitrary amplitude the resultant velocity field $\mathbf{v}$ is an exact solution of the Navier–Stokes equations. The disturbance is written as

$$\mathbf{v}' = \hat{\mathbf{v}}(t)F(\eta) \quad \text{where} \quad \eta = \boldsymbol{\alpha}(t).\mathbf{x} + \delta(t), \tag{4.95}$$

and the quantities α and δ are chosen such that

$$\frac{\mathrm{d}\boldsymbol{\alpha}}{\mathrm{d}t} + \mathbf{S}^T\boldsymbol{\alpha} = \mathbf{0} \quad \text{and} \quad \frac{\mathrm{d}\delta}{\mathrm{d}t} + \boldsymbol{\alpha}.\mathbf{V}_0 = 0.$$

From (4.95) the continuity equation (1.12) is satisfied provided $\hat{\mathbf{v}}.\boldsymbol{\alpha} = 0$ and making use of that and, furthermore, setting

$$F(\eta) = A\cos K\eta + B\sin K\eta,$$

where A, B, K are constants, Craik and Criminale show that, when the body force is zero, $\hat{\mathbf{v}}$ satisfies

$$\frac{\mathrm{d}\hat{\mathbf{v}}}{\mathrm{d}t} + \mathbf{S}\hat{\mathbf{v}} = -\nu K^2\boldsymbol{\alpha}.\boldsymbol{\alpha}\hat{\mathbf{v}} + 2\mathbf{T}\hat{\mathbf{v}}/\boldsymbol{\alpha}.\boldsymbol{\alpha} \tag{4.96}$$

where, with $\boldsymbol{\beta} = \mathbf{S}^T\boldsymbol{\alpha}$, $\mathbf{T} = (\beta_1\boldsymbol{\alpha}, \beta_2\boldsymbol{\alpha}, \beta_3\boldsymbol{\alpha})$.

Although formulated generally, Craik and Criminale consider steady basic flows such that $\mathbf{S}$, $\mathbf{V}_0$ are constant. In particular they concentrate on two-dimensional flows with

$$\mathbf{S} = \begin{pmatrix} 0 & 0 & 0 \\ 0 & a & b \\ 0 & -b & -a \end{pmatrix}, \tag{4.97}$$

and three-dimensional flows with

$$\mathbf{S} = \begin{pmatrix} a & 0 & 0 \\ 0 & b & 0 \\ 0 & 0 & -a-b \end{pmatrix}. \tag{4.98}$$

In (4.97) the degenerate case $a = \pm b$ corresponds to the problem addressed by Kelvin (1887) but in a different co-ordinate frame. Kelvin's shear matrix is

$$\mathbf{S} = \begin{pmatrix} 0 & 0 & k \\ 0 & 0 & 0 \\ 0 & 0 & 0 \end{pmatrix},$$

for which $\boldsymbol{\alpha} = \{\alpha_1, \alpha_2, \alpha_3(t)\}$ where α_1, α_2 are constants and $\alpha_3(t) = \alpha_3(0) - k\alpha_1 t$. The solution of (4.94) for the third component may then be written as

$$\hat{w}(t) = \exp\left[-\frac{\nu K^2}{3k\alpha_1}\{3k\alpha_1(\alpha_1^2 + \alpha_2^2)t - \alpha_3(t)^2\}\right] / \boldsymbol{\alpha}.\boldsymbol{\alpha},$$

and $\hat{u}$, $\hat{v}$ follow by direct integration. This particular case was first considered by Kelvin, who was apparently unaware of its status as an exact solution of the Navier–Stokes equations believing that $|\mathbf{v}'| \ll 1$ was a necessary condition for the disturbance.

Craik and Criminale also discuss two-dimensional flows, (4.97), for $a^2 \neq b^2$, $a = 0$ and $b = 0$; and for three-dimensional flows, (4.98), for $a = b$, $2a + b = 0$ and $a + 2b = 0$.